Agricultural and Forest Meteorology 350 (2024) 109951

Contents lists available at ScienceDirect

Agricultural and Forest Meteorology

journal homepage: www.elsevier.com/locate/agrformet

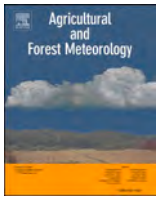

A brief history of the thermal IR-based Two-Source Energy Balance (TSEB) model – diagnosing evapotranspiration from plant to global scales

Martha C. Anderson [a,*], William P. Kustas [a], John M. Norman [b], George T. Diak [p], Christopher R. Hain [c], Feng Gao [a], Yun Yang [d], Kyle R. Knipper [e], Jie Xue [a], Yang Yang [f], Wade T. Crow [a], Thomas R.H. Holmes [g], Hector Nieto [h], Radoslaw Guzinski [q], Jason A. Otkin [i], John R. Mecikalski [j], Carmelo Cammalleri [k], Alfonso T. Torres-Rua [l], Xiwu Zhan [m], Li Fang [m], Paul D. Colaizzi [n], Nurit Agam [o]

[a] *Hydrology and Remote Sensing Laboratory, USDA-ARS, Beltsville, MD, United States*
[b] *University of Wisconsin, Madison, WI, United States*
[c] *NASA Marshall Space Flight Center, Huntsville, AL, United States*
[d] *Mississippi State University, Starkville, MS, United States*
[e] *Sustainable Agricultural Water Systems, USDA-ARS, Davis, CA, United States*
[f] *Beijing Normal University, Zhu Hai, China*
[g] *NASA Goddard Space Flight Center, Greenbelt, MD, United States*
[h] *Institute of Agricultural Sciences, CSIC, Madrid, Spain*
[i] *Space Science and Engineering Center, University of Wisconsin, Madison, WI, United States*
[j] *University of Alabama-Huntsville, Huntsville, AL, United States*
[k] *Politecnico di Milano, Dipartimento di Ingegneria Civile e Ambientale (DICA), Milan, Italy*
[l] *Utah Water Research Laboratory, Utah State University, Logan, UT, United States*
[m] *NOAA NESDIS, College Park, MD, United States*
[n] *Conservation and Production Research Laboratory, USDA-ARS, Bushland, TX, United States*
[o] *Blaustein Institutes for Desert Research, Ben-Gurion University of the Negev, Israel*
[p] *Space Sciences and Engineering Center, University of Wisconsin, Madison, WI, United States*
[q] *DHI GRAS, Hørsholm, Denmark*

ARTICLE INFO

Keywords:
Evapotranspiration
Thermal infrared
Land-surface temperature
Remote sensing
Surface energy balance

ABSTRACT

Thermal infrared (TIR) remote sensing of the land-surface temperature (LST) provides an invaluable diagnostic of surface fluxes and vegetation state, from plant and sub-field scales up to regional and global coverage. However, without proper consideration of the nuances of the remotely sensed LST signal, TIR imaging can give poor results for estimating sensible and latent heating. For example, sensor view angle, atmospheric impacts, and differential coupling of soil and canopy sub-pixel elements with the overlying atmosphere can affect the use of satellite-based LST retrievals in land-surface modeling systems. A concerted effort to address the value and perceived shortcomings of TIR-based modeling culminated in the Workshop on Thermal Remote Sensing of the Energy and Water Balance, held in La Londe les Maures, France in September of 1993. One of the outcomes of this workshop was the Two-Source Energy Balance (TSEB) model, which has fueled research and applications over a range of spatial scales.

In this paper we provide some historical context for the development of TSEB and TSEB-based multi-scale modeling systems (ALEXI/DisALEXI) aimed at providing physically based, diagnostic estimates of latent heating (evapotranspiration, or ET, in mass units) and other surface energy fluxes. Applications for TSEB-based ET retrievals are discussed: in drought monitoring and yield estimation, water and forest management, and data assimilation into – and assessment of – prognostic modeling systems. New research focuses on augmenting temporal sampling afforded in the thermal bands by integrating cloud-tolerant, microwave-based LST information, as well as evaluating the capabilities of TSEB for separating ET estimates into evaporation and transpiration components. While the TSEB has demonstrated promise in supplying water use and water stress information down to sub-field scales, improved operational capabilities may be best realized in conjunction with

* Corresponding author.
E-mail address: martha.anderson@usda.gov (M.C. Anderson).

https://doi.org/10.1016/j.agrformet.2024.109951
Received 1 November 2023; Received in revised form 15 February 2024; Accepted 26 February 2024

ensemble modeling systems such as OpenET, which can effectively combine strengths of multiple ET retrieval approaches.

1. Introduction

Numerous studies have demonstrated that land-surface temperature (LST) is a valuable diagnostic indicator of vegetation moisture status and energy balance. Indeed, a recent state-of-the-art review paper by García-Santos et al. (2022) contains over 240 citations of thermal-based model development and validation studies published over the last 30 years. The value of canopy temperature for evapotranspiration (ET) estimation was recognized nearly 50 years ago in a publication by Brown (1974) in this journal before it was renamed *Agricultural and Forest Meteorology* in 1985. Although no single modeling approach is identified as superior when reviewing all the validation studies, the utility of thermal-based methods is strongly promoted by projects such as OpenET, which is developing an operational ensemble ET product for water management (Melton et al., 2022).

This has not always been the case. Thermal infrared (TIR) imaging sensors were at one point eliminated from the design of Landsat 8 (then, the Landsat Data Continuity Mission), as they were deemed too expensive and not widely used (Irons et al., 2012). Results from some earlier field experiments, including the First ISLSCP (International Satellite Land-Surface Climatology Project) Field Experiment (FIFE) of 1987, suggested poor agreement of thermal energy balance models with observed fluxes, yielding large scatter and bias. These results showed that the relationship between the surface-to-air temperature gradient and sensible heat flux varied widely based on atmospheric conditions, vegetation cover, sensor view angle, and other factors, and hence was not deemed a viable approach for surface energy balance estimation (Hall et al., 1992; Vining and Blad 1992).

And yet, at around the same time as FIFE, there was ongoing work demonstrating that LST *can* be meaningfully interpreted within the context of complexities within the soil-plant-atmosphere continuum (SPAC). Detailed models were used to describe the radiation and turbulent energy exchange within the SPAC (Norman 1979; Norman and Campbell, 1983; Norman 1988), resulting in the determination of effective soil and canopy temperatures that could be used in thermal-based modeling approaches. There were also temporal surface temperature scaling methods being developed by Wetzel et al. (1984) and Diak and Whipple (1993) and contextual ET methods (Bastiaanssen et al., 1998; Allen et al., 2007) that aimed at reducing sensitivity to errors in satellite-based LST retrieval.

A concerted effort to address the value and perceived shortcomings of TIR-based modeling culminated in the Workshop on Thermal Remote Sensing of the Energy and Water Balance over Vegetation in Conjunction with Other Sensors, held in La Londe les Maures, France, in September of 1993 (Carlson et al., 1995).The findings of the workshop helped to design a way forward in the application of TIR imaging for energy balance and ET modeling.

One of the outcomes of the La Londe workshop was the Two-Source Energy Balance (TSEB) model (Norman et al., 1995b), which has since fueled a wide range of research and applications over many spatial scales. In this paper we provide some historical context (see chronology in Table 1) for the development of TSEB and TSEB-based modeling systems (ALEXI/DisALEXI) and discuss new implementations and applications for these models.

2. Early history of TIR-Based ET modelling

2.1. TIR as an indicator of surface moisture status

Monteith and Szeicz (1962) and Tanner (1963) were among the first to use infrared thermometry to determine soil and plant temperatures. Monteith and Szeicz (1962) noted the view-angle and solar-angle effects on radiative temperature observations, measuring over both short and tall crops as well as bare soil and water surfaces. They concluded that "When the aerodynamic character of a crop is known, the effective resistance of the stomata to water-vapour diffusion can be related theoretically to the difference between surface and air temperature." Tanner (1963) noted that "Though these data are incomplete, they do support a conviction the author has held since beginning micrometeorological work about 7 years ago – that plant temperature may be a valuable qualitative index to differences in plant water regimes. Coupled with a better understanding of transfer processes at the plant surfaces, they may serve to provide quantitative data on plant-water status."

A significant advancement in the application of TIR temperature for estimating plant water use and stress came from the work of Jackson et al. (1977) and Idso et al. (1977), who used canopy-air temperature differences as an indicator of crop water requirements. These studies, however, neglected other environmental factors that affect atmospheric demand; namely, vapor pressure deficit (VPD), wind, and radiation. Idso et al. (1981) derived an empirical method based on the temperature difference-VPD relationship for quantifying stress by determining "non-water-stressed baselines" for crops. These baselines defined the lower limit of the canopy temperature that a particular crop canopy would attain if the plants were transpiring at their potential rate, although the upper temperature limit for a non-transpiring crop was ill-defined in this method. Jackson et al. (1981; R.D. 1988) took this a step further and incorporated the plant energy balance along with the Penman-Monteith (PM) expression for canopy transpiration to derive a formulation of the canopy-air temperature difference as a function of VPD and defined theoretically the limits associated with potential ET and when ET approaches zero. The crop water stress index (CWSI) was defined by subtracting the ratio of actual to potential ET from one, a plant moisture indicator that has been widely evaluated over different crops.

While these approaches were found to have potential, a critical limitation was their requirement of temperature measurements that sampled the canopy only (avoiding any influence from the background soil temperature) as well as in-situ measurements of the local meteorological conditions. This made them difficult to scale from the canopy level to the whole field or landscape and regional scales. Around the same time as the development of the CWSI, others were investigating the potential of aircraft and satellite TIR data to provide large-area estimates of ET. Bartholic et al. (1972) flew a scanning spectrophotometer with a TIR band for measuring LST variations in soils and crops at various water availability levels. Price (1980) used analytical expressions relating the mean evaporation rate of a bare soil surface to satellite-derived surface temperature based on the thermal inertia concept, using a numerical model simulating the diurnal cycle of surface temperature to correct for micrometeorological drivers. Carlson et al. (1981) advanced this by including a one-dimensional boundary layer model with a single-source energy balance model, using LST as a boundary condition over urbanized landscapes. Taconet et al. (1986) was one of the first to introduce a soil-vegetation land surface scheme coupled to satellite-derived LST. While the modeled fluxes agreed with measurements taken during a dry down, sensitivity to initial boundary layer conditions and uncertainty in LST had a significant effect on model output. A few years later, Carlson et al. (1990) proposed a similar approach, but added constraints derived from a two-dimensional plot between LST and the normalized difference vegetation index (NDVI), which is related to fractional vegetation cover. From this 2D plot, the temperatures of sunlit bare soil and full cover vegetation were derived and variations between these two limits were related to the moisture availability as well fractional cover. Gillies et al.

Table 1: Chronology of events relating to TIR remote sensing and TSEB development.

	Year	Contribution
Monteith and Szeicz	1962	Early paper using TIR to determine soil and canopy temperatures
Tanner	1963	Postulates that TIR could provide plant water status
Garrat and Hicks	1973	Use of kB^{-1} parameter in computing sensible heat (H) from LST with a single-source approach
Jackson et al.	1977	TIR is related to crop water requirements
Price	1980	Use of thermal inertial concept to estimate bare soil evaporation
Jackson et al.	1981	Introduction of the crop water stress index (CWSI)
Carlson et al.	1981	Couples LST and 1D atmospheric boundary layer (ABL) model to assess moisture status
Seguin and Itier	1983	Extends one-time-of-day LST to daily using semi-empirical transfer eq.
Wetzel et al.	1984	Relates LST change from GOES and ABL growth to soil moisture
Shuttleworth & Wallace	1985	Develops a two-source approach for sparse canopies
Taconet et al.	1986	Introduces a coupled soil-vegetation-atmosphere transfer (SVAT)-ABL model linked to satellite-derived LST
FIFE	1987	Tested LST-flux relations in a tall-grass prairie
Diak and Stewart	1989	Uses diurnal LST variations from GOES to derive surface energy fluxes
Carlson et al	1990	Uses a SVAT-ABL coupled model constrained by 2D plot of LST & NDVI
Hall et al.	1992	Concludes TIR-based H estimation is infeasible, based on FIFE data
La Londe Workshop	1993	In part a response to the FIFE findings on the utility of LST
Moran et al.	1994	Uses 2D plot of LST-NDVI to extend CWSI to partial canopy cover
Norman, Kustas et al.	1995	First publication on the TSEB
Anderson et al.	1997	First publication on ALEXI (originally TSTIM)
Norman et al.	2000	Introduces Dual-Temperature-Difference approach using TSEB
Norman et al.	2003	First publication on DisALEXI
Kustas et al	2003	Proposes method of sharpening coarser LST with finer resolution NDVI
Allen et al.	2005	Use of Landsat ET for water management in the western U.S.
Gao et al.	2006	Spatial Temporal Adaptive Reflectance Fusion Model (STARFM)
Anderson et al.	2007	Introduction of the Evaporative Stress Index (ESI)
	2008	USGS announces free-and-open Landsat data policy
	2009	NASA approves build of TIRS for Landsat 8
Gao et al.	2012	Introduction of the TIR Data Mining Sharpener (DMS)
Cammalleri et al.	2013	STARFM applied to ET data fusion
Colaizzi et al.	2014	Incorporates Penman-Monteith (PM) transpiration formula in TSEB
Hain et al.	2017	Describes MODIS-based global ALEXI, launched at NASA-Marshall
Holmes et al.	2018	Uses microwave-based LST in ALEXI to improve cloud tolerance
Fang et al.	2019	Describes GET-D system operating at NOAA-NESDIS
Nieto et al.	2019	Improves radiation modeling of row crops in TSEB
Li et al.	2019	New soil resistance formulation proposed in TSEB for sparse canopies
Guzinski et al	2020	Sen-ET for global applications using Sentinel 2 & 3 satellites
Anderson et al.	2021	Demonstrates multi-source ET fusion to improve temporal sampling
Melton et al.	2022	OpenET launched
Burchard-Levine et al.	2022	Modifies TSEB to 3SEB for understory veg in tree/vine-grass systems
Xue et al.	2022	GOES, Landsat, Sentinel-2, ECOSTRESS, and VIIRS data fusion
Knipper et al.	2023	E & T partitioning with DisALEXI and PM over woody perennials

(1997) later verified the Carlson et al. (1990) methodology, coined the "triangle method", with flux data from FIFE, conducted in Manhattan, KS, and the Monsoon 90 experiment in Walnut Gulch, AZ. They pointed out that this approach, as well as others using soil-plant models coupled to the atmospheric boundary layer, are solving the so-called inverse problem, which is defined as fitting a measured variable to a simulated (modeled) value such that a solution is reached when the simulated and observed values are equal within some pre-defined uncertainty level for soil water content or surface fluxes. Model inversion is a standard practice in remote sensing and is also applied, for example, in retrieving leaf area index and other biophysical properties from multi-spectral reflectance data (Houborg et al., 2007) and atmospheric profiles from sounder observations (Menzel et al., 2018).

2.2. One-source energy balance modeling: kB^{-1} and R_{EX}

About the same time in the mid 1990's, another focus of research in TIR-based energy balance was on determining robust formulations for resistances relating vertical temperature gradients to sensible heat flux, and for relating the observed directional radiometric surface temperature, $T_R(\theta)$, obtained at viewing angle θ, to the "aerodynamic temperature for heat", T_O (K), which satisfies the bulk resistance formulation for sensible heat transport, H:

$$H = \rho C_P \frac{(T_O - T_A)}{R_A + R_{EX}} = \rho C_P \frac{(T_O - T_A)}{R_{AH}} \quad (1)$$

Here, H is the sensible heat flux (W m^{-2}), ρ is air density (kg m^{-3}), C_p is the heat capacity of air (J kg^{-1} K^{-1}), T_A is the air temperature in the surface layer measured at some height above the canopy (K), R_{EX} is an excess resistance associated with heat transport (s m^{-1}), R_A is the aerodynamic resistance (s m^{-1}), and is typically estimated in the surface layer using a stability corrected logarithmic formula (Brutsaert 1982):

$$R_A = \frac{\left[1n\left(\frac{z_U - d_o}{z_{oM}}\right) - \psi_M\right]\left[1n\left(\frac{z_T - d_o}{z_{oM}}\right) - \psi_H\right]}{k^2 u} \quad (2)$$

while $R_{AH} \equiv R_A + R_{EX}$ is the total resistance to heat transport across the temperature gradient T_O–T_A. In Eq. (2), k is von Kármán's constant (~ 0.4), d_O is the displacement height (m), z_{OM} is the roughness length for momentum transport (m), u is the wind speed (m s^{-1}) measured at height z_U (m), z_T (m) is the height of the T_A measurement, and Ψ_M and Ψ_H are the Monin-Obukhov stability functions for momentum and heat, respectively.

The excess resistance term in Eq. (1) captures the fact that heat must diffuse through the laminar boundary layers of the canopy and soil elements, while the transfer of momentum is much more efficient as a result of viscous shear and form drag of the vegetation and soil elements

involving local pressure gradients. This difference in transport mechanisms for heat and momentum is often defined as a difference in effective roughness length; namely, $R_{EX} = [\ln(z_{OM}/z_{OH})]/[k\ u_*]$, where z_{OH} is the roughness length for heat transport and u_* is the friction velocity; $u_* = u\ k/[\ln(z_U - d_O)/z_{OM} - \Psi_M]$.Typically, z_{OH} is approximated as a fraction of z_{OM} (~ 0.1 z_{OM}). There has been considerable effort to evaluate z_{OH} or the ratio $\ln(z_{OM}/z_{OH}) = kB^{-1} = k\ u_*\ R_{EX}$ (Garrat and Hicks 1973; Kustas et al., 1989; Stewart et al., 1994) for different surfaces, employing $T_R(\theta)$ observations and measurements of most of the variables in Eqs. (1) and (2). Here, B is a shorthand symbol representing the interfacial scalar transport coefficient proposed by Owen and Thompson (1963).

When $T_R(\theta)$ is used in Eq. (1) instead of T_O with measured fluxes to estimate the roughness length for heat, the theoretical framework that defined z_{OH} is modified and referred to as the "radiometric roughness length" z_{OR} (e.g., Brutsaert and Sugita 1996). Studies evaluating z_{OR} find significant scatter in resulting values and no single formulation can clearly explain the observed variation, which is especially evident for unclosed canopies with partial vegetation cover (e.g., Stewart et al., 1994; Sun and Mahrt 1995; Kustas et al., 1996; Verhoef et al., 1997; Troufleau et al., 1997). Apparently too many factors affect z_{OR} for it to be a useful working approach. Blyth and Dolman (1995) applied a two-source modeling approach that treats the land surface as a composite of soil and canopy elements and found the dependence of z_{OH} (z_{OR}) on a variety of surface conditions that included fractional vegetation cover, soil and vegetation resistances, as well as on the available energy at the surface (difference between net radiation and soil heat flux or R_N - G), and humidity deficit. A similar result was obtained by Lhomme et al. (1997) using the two-source model originally developed by Shuttleworth and Wallace (1985). Even more disconcerting was that observational and modeling studies show a dependency of z_{OR} on radiometer viewing angle, θ (Vining and Blad 1992; Matsushima and Kondo 1997), adding complexity to the retrieval of surface energy balance using radiometric temperature data acquired off-nadir.

Some have examined approaches that avoid parameterization of z_{OR} (e.g., assuming $R_{EX} = 0$ or a constant in Eq. (1)), and instead use semi-empirical formulations to account for the difference between T_O and T_R which, it is argued, can be more accurately applied to observational data (e.g., Lhomme et al., 1994; Chehbouni et al., 1996; Mahrt et al., 1997; Sun et al., 1999). However, these formulations are typically calibrated with experimental data, and hence may be difficult to transfer *a priori* to different land cover types (Merlin and Chehbouni 2004).

2.3. LST time differencing and integration with ABL

A third line of research at this time addressed the issue mentioned earlier by Taconet et al. (1986) concerning the sensitivity of flux estimation to the accuracy of LST. One of the first efforts using time changes in radiometric surface temperature (DT_R) to estimate land surface energy balance characteristics was by Wetzel et al. (1984), who developed a statistical method using a surface/atmospheric boundary layer (ABL) model and a series of model runs to create a simulated surface temperature dataset and soil moisture retrieval algorithm. While the purpose of this algorithm was to evaluate soil moisture, using the energy-conserving surface/ABL model to generate a DT_R dataset meant that the surface energy balance was implicit in the resulting soil moisture retrieval. It was shown that the method performed best over bare surfaces or with minimal vegetation and not as well over more densely covered vegetated surfaces.

The concept of integrating a surface and mixed layer model with diurnal LST variations from geostationary satellites to derive daily surface energy fluxes was proposed by Diak and Stewart (1989) and Diak (1990). They developed a soil/surface/ABL model that was initialized with atmospheric profiles measured at radiosonde stations and combined with geostationary measurements of DT_R to evaluate the surface energy balance (Bowen ratio, B_o: the dimensionless ratio of sensible to latent heat) at the radiosonde locations. These stations, distributed across the U.S., had surface conditions ranging from densely vegetated and very wet to arid, with sparse or little to no vegetation. Results were consistent with station climatology. This study also demonstrated the very high correlation between daytime surface sensible heating and the time change of the height of the ABL, both using the theoretical atmospheric model in a so-called "forward" mode (incident solar radiation amounts and values of B_o were varied and DT_R generated) and also with comparisons of the ABL vertical structure from the radiosonde profiles to the model-driven ABL profiles forced by the actual DT_R measurements.

Similarly, the study of Diak and Whipple (1993) used DT_R measurements, radiosonde atmospheric profiles, and the soil/surface/ABL model to evaluate both the Bowen ratio and an "effective" surface roughness length (z_O) across the same radiosonde stations. Once again, z_O and B_o results were consistent with the surface climatology of these stations. Diak and Whipple (1994) demonstrated that observed time changes in ABL height themselves are predictive of time-integrated sensible heat flux. Other studies of the era also established the utility of the combined use of DT_R and surface/ABL structure to provide surface forcing and SEB closure (Gillies et al., 1997), the sensitivity of ABL growth to daytime sensible heating already having been well established.

3. TIR challenges: from FIFE to La Londe

3.1. FIFE

The First ISLSCP (International Satellite Land-Surface Climatology Project) Field Experiment (FIFE) was conducted in 1987 in the Konza Prairie outside of Manhattan, Kansas (Sellers et al., 1988). The main goal of FIFE was to understand the role of the vegetated land surface in controlling the exchange of water, energy and carbon fluxes with the lower atmosphere or boundary layer and the utility of satellite observations to quantify climatologically significant land surface parameters and fluxes. This was an interdisciplinary effort involving researchers in plant physiology, meteorology, micrometeorology, hydrology, and remote sensing. Some of the early TIR methods discussed above were tested using FIFE measurements, collected over a tall-grass prairie landscape.

Many scientific gains were obtained from FIFE studies of the ABL, surface fluxes, TIR correction and calibration, surface radiance and biology, soil moisture, and integrative science (Sellers et al., 1988). However, some so-called "failures and unresolved issues" of solving the surface energy balance using satellite remote sensing were also identified, as documented by Hall et al. (1992). One of these reported failures regarded the utility of LST in constraining heat fluxes, based on $T_R(\theta)$ observations collected by a helicopter-mounted modular multispectral radiometer. Comparisons of T_O derived from eddy covariance tower measurements of H (using Eq. (1)) with $T_R(\theta)$ exhibited significant scatter. Moreover, Hall et al. (1992), using the observed $T_R(\theta)$ directly in Eq. (1) without accounting for an excess resistance term, showed significant scatter with H measured at the eddy covariance towers ($R^2 = 0.45$). They also pointed out that the study by Vining and Blad (1992), using ground-based TIR radiometers with varying viewing angles of the surface, was not able to identify a consistently optimal viewing angle where $T_R(\theta)$ would approximate T_O, as needed to compute H. The fundamental difference between $T_R(\theta)$ and T_O as defined by Eq. (1) led Hall et al. (1992) to conclude: "Unfortunately, from our research we also found that the remote estimation of surface temperature to useful accuracies is problematical; consequently, the use of thermal infrared measurements to infer sensible heat flux is probably not feasible to acceptable accuracies."

Questions regarding the utility of TIR stemming from FIFE and related studies were one reason why a thermal band sensor was originally omitted from plans for the Landsat Data Continuity Mission being developed in the 1990s, a decision that was later reversed as TIR-based applications in water management started to flourish (Irons et al., 2012).

3.2. La londe workshop

The conclusions from the Hall et al. (1992) paper regarding the utility of TIR remote sensing for surface energy balance estimation was a key factor leading to the La Londe Workshop in 1993. The goal of the workshop was to foster discussion of various methods using TIR observations for deriving land surface states and fluxes from plant to field and regional scales, resulting in special issues in *Agricultural and Forest Meteorology* and in *Remote Sensing Reviews*. The overview paper by Carlson et al. (1995) summarized the key findings of the workshop.

The workshop was organized around five topics addressing different issues (such as thermal emissivity, atmospheric correction, angular effects) affecting the practical use of thermal remote sensing. One of the important outcomes of the workshop was an overview paper that outlined a consistent terminology for thermal infrared remote sensing (Norman and Becker 1995). However, the most deeply discussed topic was the application of the excess resistance term (i.e. R_{EX}), which was recognized as essential for reconciling the differences between aerodynamic and radiometric surface temperature. The workshop concluded that "Reasonably accurate calculations of surface energy fluxes can be made using infrared temperatures provided that appropriate values for the so-called extra resistance (expressed in terms of kB^{-1}) are used. It is understood, however, that the extra resistance is a theoretical artifact which is correctly applied only over homogeneous surfaces and not over a partial vegetation cover, especially those surfaces with distinctly separate vegetation and bare soil patches; the factor should be employed separately for vegetation and bare soil regimes." In other words, it became clear that for partial canopy cover conditions having both bare soil and canopy temperatures in the radiometer footprint, the use of a single-source resistance formulation was tenuous without some type of calibration for this excess resistance term.

This latter comment was implicitly suggesting that the resistance to heat transport from the soil and vegetation needed to be treated differently, and a conceptual framework for doing this with radiometric surface temperature was initially proposed at the workshop by John Norman in a schematic diagram (Fig. 1). This type of modeling scheme is related to the formulations using the Penman-Monteith equation developed by Shuttleworth and Wallace (1985) and later by Shuttleworth and Gurney (1990), relating the soil and canopy aerodynamic and water vapor resistance to soil and canopy temperatures. It should be mentioned that Kustas (1990) also attempted to apply a two-source (two-layer) approach using radiometric temperatures to a sparse canopy system. However, that two-source modeling scheme had an *ad hoc* approach for quantifying the soil evaporation component that proved to cause measurable uncertainty in the output of ET. The new formulation could effectively achieve a solution for both the energy and radiative temperature balance of the surface (see below).

Another major topic of discussion at La Londe was the recognition that the uncertainty in LST from satellites, which may be on the order of 2–3 K, can be problematic for surface energy balance estimates over landscapes having relatively small surface-air temperature differences. The time-differencing techniques described by Diak at the workshop offered a means to minimize the impact of LST uncertainties. This work set the stage for the application of Norman's scheme at regional scales.

3.3. The 8 challenges

Following the La Londe Workshop, Kustas, Norman, and Diak continued their discussions on how to effectively use TIR data in a physically based model of surface fluxes that would be applicable over a wide range of landcover conditions. Kustas and Norman (1996) tabulated 8 Key Challenges in using satellite retrievals of LST, stemming from the La Londe workshop. These are summarized here:

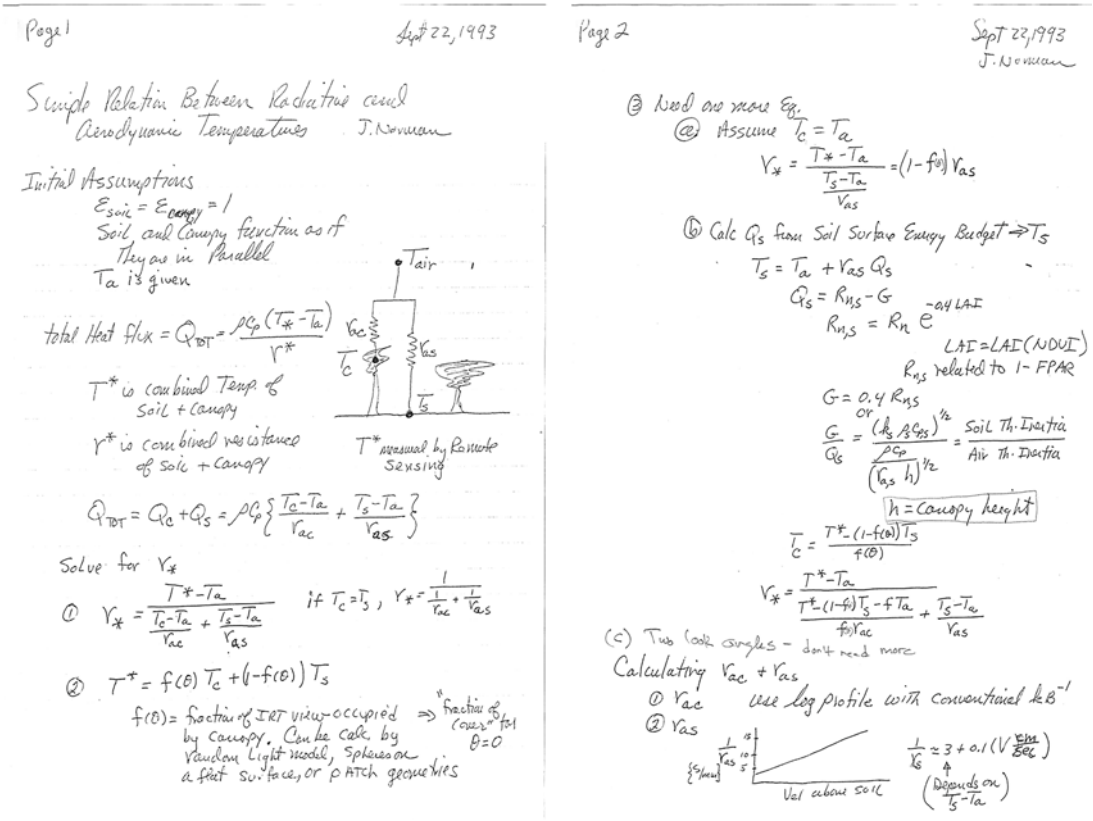

Fig. 1. Original notes on TSEB model structure, developed during the La Londe Workshop.

1. Radiometric surface temperature is not the same as the aerodynamic temperature, T_O, used in Eq. (1) to compute sensible heat.
2. Surface gradient models are sensitive to errors in air temperature measurements, which are unlikely to be consistent with the surface temperature measurements.
3. Radiometric surface temperature can have a strong dependence on view angle over partial vegetation cover.
4. Thermal emissivity is only approximately known at the image pixel scale.
5. Atmospheric and satellite corrections contribute significant errors to surface temperature.
6. Remote observations are typically instantaneous – how to scale up to daily and longer timescales?
7. Satellites with good temporal coverage tend to have large (potentially heterogeneous) pixels (and conversely, higher resolution sensors tend to have lower temporal revisit).
8. Satellite TIR observations of the Earth's surface are limited to clear-sky conditions.

The TSEB family of models was developed in response to these 8 Challenges, building on the new collaborations that emerged from La Londe.

4. . TSEB modeling frameworks

4.1. TSEB: the Two-Source Energy Balance model

The alternative approach to modeling the surface energy fluxes using LST as the boundary condition suggested by Norman (Fig. 1) considers the radiometric surface temperature (T_R) to be a composite of the soil and vegetation canopy temperatures (T_s and T_C , respectively), defined by the fractional vegetation cover (f_C) and the thermal radiometer viewing angle (θ), namely:

$$T_R(\theta) \approx \left[f_C(\theta)T_C^4 + (1-f_C(\theta))T_S^4\right]^{\frac{1}{4}} \quad (3)$$

This addresses Challenge 3, accounting for the fact that a partially vegetated scene will appear cooler (more dominated by vegetation) when viewed off-nadir. Norman et al. (1995b) gave a simple exponential expression for estimating f_C(θ) based on the leaf area index and radiometer viewing angle, which was further modified for vegetation clumping effects (Anderson et al., 2005). The partitioned soil and canopy temperatures are used in estimating the energy balance of the soil and vegetated canopy sources:

$$R_{NS} = H_S + LE_S + G \quad (4)$$

$$R_{NC} = H_C + LE_C \quad (5)$$

where R_{NS} is net radiation at the soil surface, and R_{NC} is net radiation divergence within the vegetated canopy layer, H_C and H_S are canopy and soil sensible heat flux, respectively, LE_C is the canopy latent heat flux, LE_S is soil latent heat flux, and G is the soil heat conduction flux. Weighting of the heat flux contributions from the canopy and soil components is governed by the partitioning of the net radiation between soil and canopy and by the resistance terms described below (see Kustas and Norman, 1999a). The net radiation partitioning between the soil and vegetation canopy was originally formulated by Norman et al. (1995b) using the Beer's law approximation, but was later modified to accommodate differences in shortwave and longwave radiation divergence through the canopy layer (Kustas and Norman 2000) and radiation divergence in row crops (Colaizzi et al., 2012a). A conceptual diagram of the TSEB is shown in the central panel of Fig. 2.

Norman originally suggested a parallel resistance formulation for the heat flux computation from the soil and canopy surfaces (Fig. 1), but also developed a series resistance approach, allowing interaction between the soil and canopy fluxes, that has been more commonly adopted (Fig. 2b). For the sensible heat flux from the canopy (H_C) and soil (H_S), the series gradient-resistance equations are as follows:

$$H_C = \rho C_P \frac{T_C - T_{AC}}{R_X} \quad (6)$$

$$H_S = \rho C_P \frac{T_S - T_{AC}}{R_S} \quad (7)$$

Combining H_C and H_S for the total H yields:

$$H = \rho C_P \frac{T_{AC} - T_A}{R_A} \quad (8)$$

where the variable T_{AC} is the temperature in the canopy-air space and is associated with the aerodynamic temperature, T_0. The variable R_X is the total boundary layer resistance of the complete canopy of leaves, R_S is the aerodynamic resistance to sensible heat exchange from the soil surface, and R_A is aerodynamic resistance as given in Eq (1). The original resistance formulations are described in Norman et al. (1995b). Since then, there have been revisions mainly for the R_S term (Kustas and Norman 1999b, 2000; Kustas et al., 2016; Li et al., 2018, 2019). These formulations for R_S and R_X essentially account for the excess resistance parameterizations defined in Eq. (1), namely R_{EX}, and are a more physically based representation of the soil and vegetated canopy aerodynamic properties influencing the rate of turbulent heat exchange at given soil and canopy temperatures and their gradient with the canopy-air and overlaying air temperature (Challenge 1).

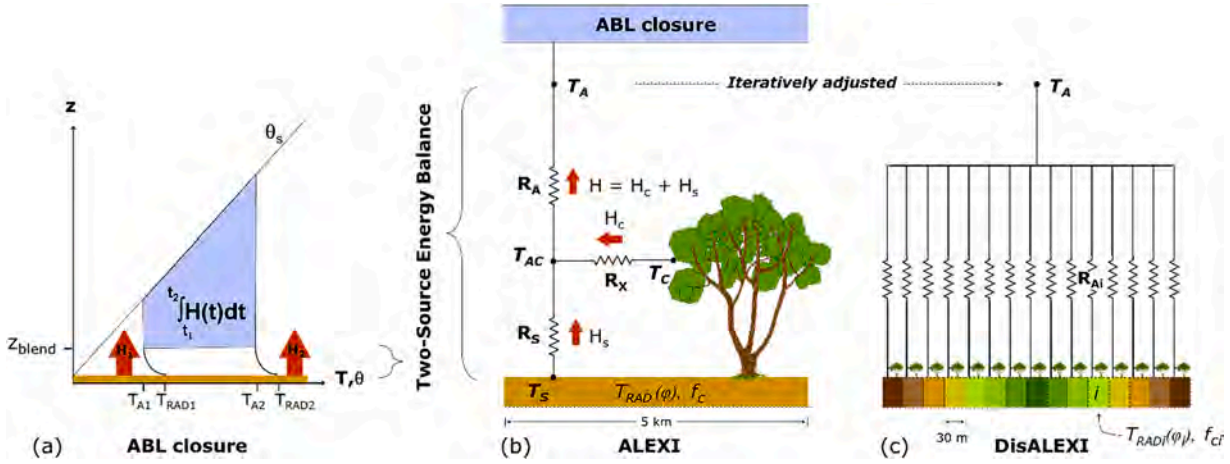

Fig. 2. Schematic diagram of the TSEB (b), ALEXI (a and b), and DisALEXI (c) models.

To achieve a closed-form solution to the set of TSEB equations, a method for estimating the plant transpiration under the inferred stress conditions was required. Norman et al. (1995b) proposed the use of the Priestley-Taylor formula for a first guess at an unstressed value of LE_C:

$$LE_C = \alpha_{PTC} f_G \frac{\Delta}{\Delta + \gamma} R_{NC}, \quad (9)$$

where α_{PTC} is the Priestley-Taylor coefficient (Priestley and Taylor 1972), and was recommended to be used for row crops by Tanner and Jury (1976). In Norman et al. (1995b) α_{PTC} was set to an initial value of 1.3. The variable f_G is the fraction of green vegetation, Δ is the slope of the saturation vapor pressure versus temperature curve, and γ is the psychrometric constant (~0.066 kPa C^{-1}). Soil evaporation is computed as the residual to the overall energy budget:

$$LE_S = R_{NC} - G - H - LE_C \quad (10)$$

Under stress conditions, the TSEB can iteratively reduce α_{PTC} from its initial value by enforcing non-negative LE_S midday, as described by Kustas and Anderson (2009).

This value of initial $\alpha_{PTC} = 1.3$ has been found to work reasonably well for most crops and natural vegetation (Agam et al., 2010), but there have been exceptions; for example, under well-watered partial canopy cover conditions in advective environments where a higher value up to an α_{PTC} ~2 may be more appropriate due to high vapor pressure deficits and temperatures (Castellvi et al., 2001; Kustas and Norman 1999b). Nominal adjustment of the initial value of α_{PTC} and estimating canopy green fraction from remote sensing for different biomes has been fairly successful in oak savannas (Andreu et al., 2018b, a), the arctic tundra, and boreal forest (Cristóbal et al., 2017; 2020), and in coniferous and deciduous forests and semiarid grasslands (Guzinski et al., 2013).

There have been efforts to improve the canopy transpiration algorithm by accounting for plant physiological responses to atmospheric forcing (i.e., vapor pressure deficit). These have included a Penman–Monteith (PM) based formulation for Eq. (9) (see (Colaizzi et al., 2012b, 2014, 2016a), or light-use efficiency (LUE) parameterization that enables estimation of coupled transpiration and carbon assimilation fluxes (Anderson et al., 2008; Houborg et al., 2011; Schull et al., 2015). More recently, Kustas et al. (2022) examined an alternative minimum stomatal resistance formulation, dependent on a VPD formulation derived from the studies of Monteith (1995) and Leuning (1995), and applicable to partial canopy conditions following the Shuttleworth-Wallace sparse canopy model. Results from each of these studies suggest there is potential improvement in ET estimation, but that the most significant impact is a potential improvement in the partitioning between LE_S and LE_C (e.g., Colaizzi et al. 2016a; Knipper et al., 2023).

The soil heat flux, G, was originally estimated as a fixed fraction (0.3) of the net radiation at the soil surface based on work of Kustas and Daughtry (1990). However, this use of a constant ratio is only applicable for a few hours around solar noon; over the full daytime period, it can yield unreliable results, particularly for partial canopy cover conditions (Colaizzi et al., 2016b, 2016c). Other studies have used a time-varying sinusoidal fraction, accounting for the hysteresis between G and R_{NS} (Santanello and Friedl 2003). For vineyards, with strongly clumped canopy structure and large row spacing, Nieto et al. (2019) found the G/R_{NS} value could be better approximated for the daytime period using a double asymmetric sigmoid function. Wetlands and flooded crop fields (e.g., rice paddies) can require a higher nominal heat storage-to-net radiation ratio (~0.6) to account for the large heat capacity of water (Anderson et al., 2018).

4.2. ALEXI: the Atmosphere-Land Exchange Inverse model

One challenge in applying the TSEB over large areas (i.e., using TIR satellite imagery to obtain gridded LST values) lies in defining reasonable air temperature boundary conditions. H (and therefore LE by energy budget residual) is very sensitive to the prescribed surface-to-air temperature gradient (Norman et al., 1995a), so errors in both T_A (Challenge 2) and LST (Challenges 4 & 5) can translate to significant errors in energy budget partitioning.

The time-differencing and ABL-coupling approaches proposed by Diak and Whipple (1993) aims to reduce model sensitivity to error sources in both LST and T_A. The Atmosphere-Land Exchange Inverse (ALEXI) model (Anderson et al., 1997; 2007b; Mecikalski et al., 1999) builds off the Diak and Whipple work, with significant improvements to the description of the soil and vegetation components of the land surface using the TSEB and satellite retrievals of f_c. Additionally, the computationally intensive soil/surface/ABL model used in Diak and Whipple (1993) was replaced with a simpler parameterization of ABL growth to facilitate modeling at higher horizontal spatial resolution and with larger areal coverage.

The standard version of ALEXI uses LST retrieved from geostationary satellites at two times during the morning ABL growth period, typically at t_1=sunrise+1.5 h and t_2=local noon-1hr. TSEB is applied at those two times with initial guesses at air temperature obtained from gridded reanalysis datasets, and corresponding instantaneous sensible heat values are derived. Assuming a linear rise in H between t_1 and t_2, a time-integrated influx of sensible heat to the ABL is computed. Using a simple slab model of ABL development (McNaughton and Spriggs 1986), the rise in boundary layer height (z_i) and potential air temperature in the mixed layer ($\theta_{mi} = T_{Ai} * \left[\frac{100}{p}\right]^{R/c_p}$) resulting from this sensible heat flux is computed as:

$$\rho c_p (z_2\theta_{m2} - z_1\theta_{m1}) = \int_{t1}^{t2} H(t)dt + \rho cp \int_{z1}^{z2} \theta_s(z)dz \quad (11)$$

based on a near-dawn potential temperature profile ($\theta_s(z)$), and new air temperature boundary conditions T_{A1} and T_{A2} are supplied to the TSEB using a nudging approach (Fig. 2a). This surface-ABL model iteration is continued until the air temperature boundaries do not significantly change. As noted by Anderson et al. (1997), the benefit of this approach is that H (and therefore LE) is primarily sensitive to time changes in LST, so time-invariant components in retrieval biases (due, e.g., to atmospheric and emissivity corrections) are removed. In addition, the air temperature boundary condition is not pre-defined via independent meteorological datasets but rather dynamically derived at the blending height interface between the surface layer and ABL modeling systems, assumed to be at 30–50 m above ground level. This boundary condition therefore responds to local forcing from spatial variability in both surface and atmospheric conditions.

Initial development with ALEXI used LST time change information from the Geostationary Operational Environmental Satellites (GOES) over the contiguous U.S. (CONUS) (Mecikalski et al., 1999; Anderson et al., 2007b), and Meteosat Second Generation (MSG) over Africa (Yilmaz et al., 2014) and Europe. Geostationary satellites are a valuable yet underutilized resource in Earth remote sensing (Khan et al., 2021). Not only do they provide diurnal information on LST, but also insolation maps (built on visible channel data) that are consistent with those LST patterns (Anderson et al., 2019) – a major benefit in regional surface energy balance, matching radiation load with thermal emission. Other primary inputs to ALEXI are obtained from moderate resolution polar-orbiting imagers (e.g., LAI, albedo) and reanalysis weather datasets (e.g., wind speed, temperature profile). A landcover map is used to assign surface roughness and canopy optical properties.

Instantaneous retrievals of LE at t_2 (LE_2) are upscaled to daily and longer totals by conserving a scaled ratio with a flux that can be estimated hourly using standard meteorological datasets. Several scaling fluxes have been tested through the years, including available energy (F_{EVAP}), reference ET (F_{RET}), and solar radiation (F_{SUN}). Of these, F_{SUN}

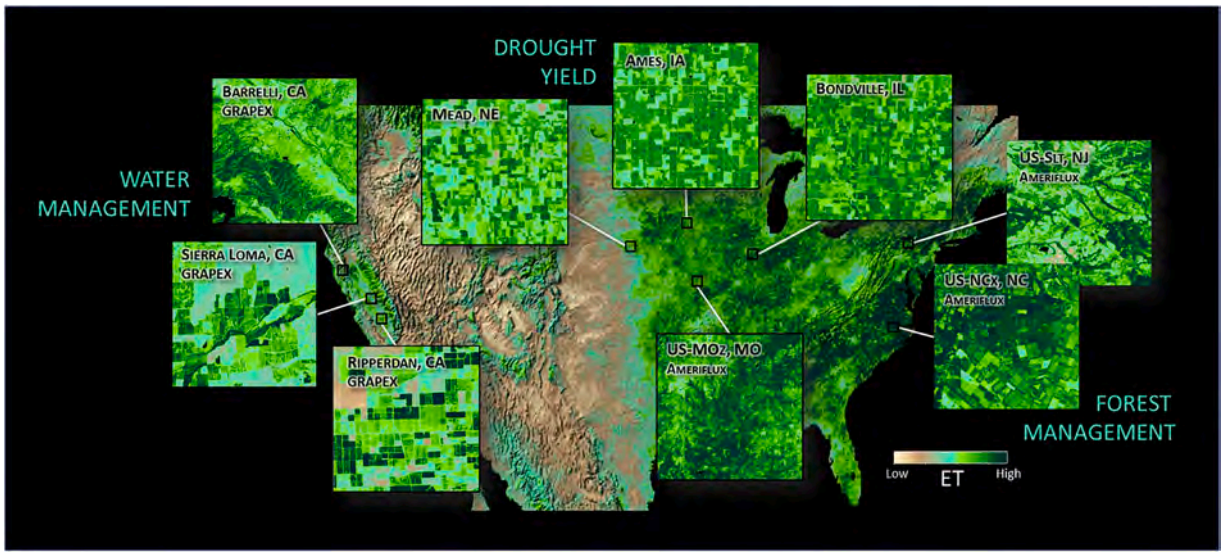

Fig. 3. Examples of 4-km ALEXI ETd over CONUS (background) and 30-m maps generated with DisALEXI, highlighting application areas described in Section 6.

has generally been found to be most conservative (least noisy) from day-to-day over a wide range of conditions (Cammalleri et al., 2014b), facilitating outlier removing, smoothing, and gap-filling of pixel-based timeseries as described by Anderson et al. (2013). F_{SUN} is currently used to generate gap-filled daily ET (ETd) maps at 4-km resolution over CONUS (see Fig. 3), while F_{RET} has proven more effective in drought-monitoring applications (Anderson et al., 2013).

It is worth noting that a simplified form of a temperature-differencing approach based on TSEB, called the Dual-Temperature-Difference (DTD) scheme, was developed for routine applications using continuous ground-based or geostationary satellite observations of LST (Norman et al., 2000; Kustas et al., 2001). The utility of DTD using proximal (Kustas et al., 2012; Vanderleest and Bland 2016) and drone LST observations (Nieto et al., 2019) or from satellite observations such as MODIS (Guzinski et al., 2013) has shown potential but has not been extensively tested.

4.3. DisALEXI: ALEXI disaggregation approach

As stated in Challenge 7, satellites with good temporal coverage tend to have lower spatial resolution. While geostationary satellite technology has improved significantly in quality and spatiotemporal resolution, the thermal band sensors are still too coarse to discern individual farm fields and landcover/management units embedded in a heterogeneous landscape. To unambiguously connect satellite retrievals with human activities and natural phenomena occurring on the ground, achieving this threshold of resolution (< 100 m) is a necessity. To reach this spatial threshold while still retaining the regional benefits afforded by LST time-differencing, an ALEXI downscaling approach (DisALEXI) was developed (Figs. 2c, 3), using the TSEB soil-plant-atmosphere coupling network to guide redistribution of ALEXI ET fluxes at a sub-pixel level (Norman et al., 2003; Anderson et al., 2004). DisALEXI has evolved over the years to accommodate new sources of TIR inputs and to be more robust over a wider range of conditions. Here, we describe the most recent implementation (see e.g., Sun et al., 2017).

In DisALEXI, the TSEB is run in a gridded mode using LST and LAI from higher resolution satellites (e.g., Landsat, MODIS, VIIRS) or airborne systems, and an initial guess at blending height air temperature from reanalysis. Upscaling to the daily timescale using F_{SUN}, TSEB ETd is aggregated over each ALEXI pixel area ($\langle$TSEB ETd$\rangle$) and compared to ALEXI ETd. The air temperature boundary over a given ALEXI pixel is nudged downward if $\langle$TSEB ETd$\rangle$ exceeds ALEXI ETd (thereby increasing the surface-to-air temperature gradient and sensible heat flux), and up-adjusted if $\langle$TSEB ETd$\rangle$ is too low. This nudging compensates for potential biases between the coarse and higher resolution LST data, e.g., due to atmospheric or angular effects, or differences in acquisition time (Anderson et al., 2021). This process iterates until $\langle$TSEB ETd$\rangle$ matches ALEXI ETd at the ALEXI pixel scale (Fig 2c). A final spatial smoothing of the resultant air temperature field is performed to eliminate discontinuities in the flux map at ALEXI pixel boundaries. The result is a map that preserves ALEXI ETd at the coarse scale, but represents subpixel variations in energy budget partitioning consistent with the high-resolution remote sensing information on LST and vegetation cover as interpreted by the TSEB.

The key inputs to DisALEXI are coarse-resolution maps of ALEXI ETd, along with LST and surface reflectance (for LAI and albedo) at moderate or high spatial resolution, and the same near-surface meteorological data used in ALEXI. With moderate resolution polar-orbiting sensors (MODIS, VIIRS), we typically have sufficient temporal coverage (near daily overpass) to gap-fill using the techniques described above for ALEXI. In this case, however, ALEXI ETd is used as the scaling flux (F_{ALEXI}) to ensure temporal consistency between the ET timeseries (Sun et al., 2017). Higher resolution thermal sensors (e.g., Landsat) generally have sampling that is temporally too sparse (8–16 day revisit) to reliably interpolate between clear-sky retrievals, especially in areas/times with persistent cloud cover. At this scale, a multi-sensor fusion approach is beneficial (see below).

5. Tools for improving spatiotemporal resolution

Challenges 7 and 8 highlight the reality that it is often difficult to obtain adequate temporal sampling for robust ET mapping at high-resolution with a single satellite thermal sensor, especially in humid regions and in landscapes undergoing rapid changes. Two approaches have been used to address these challenges: 1) augmenting Landsat sampling with other Landsat-like sensors; and 2) fusing Landsat-like sparse ET timeseries with moderate resolution temporally dense (daily) timeseries.

5.1. Thermal sharpening

While medium-to-high resolution harmonized multi-source surface reflectance (SR) datasets are available with good temporal frequency (e.g., the Harmonized Landsat-Sentinel (HLS) and Planet datasets), this is not the case with TIR datasets used to retrieve LST. Several Landsat-like thermal sensors are currently in operation (e.g., ECOsystem Spaceborne

Table 2
List of past, current, and planned Landsat-like thermal missions, along with sensor characteristics and source of complementary medium-resolution surface reflectance data.

Platform	# TIR bands	Resolution (m)	Revisit (days)	SR source (med res)	Launch date	Mission end
Landsat 4	1	120	16	On-board	1982	2001
Landsat 5	1	120	16	On-board	1984	2013
Landsat 7	1	60	16	On-board	1999	2022
Landsat 8	2	100	16	On-board	2013	
Landsat 9	2	100	16	On-board	2021	
Landsat Next	5	60	6	On-board	*2030*	
ECOSTRESS	5	70	~4	HLS	2018	
VIIRS I5	1	375	~1	HLS	2011	
Trishna	4	60	3	On-board	*2025*	
SBG	6	60–90	3	On-board	*2027*	
LSTM-A & B	5	50	2 to 3	On-board	*2029/2031*	

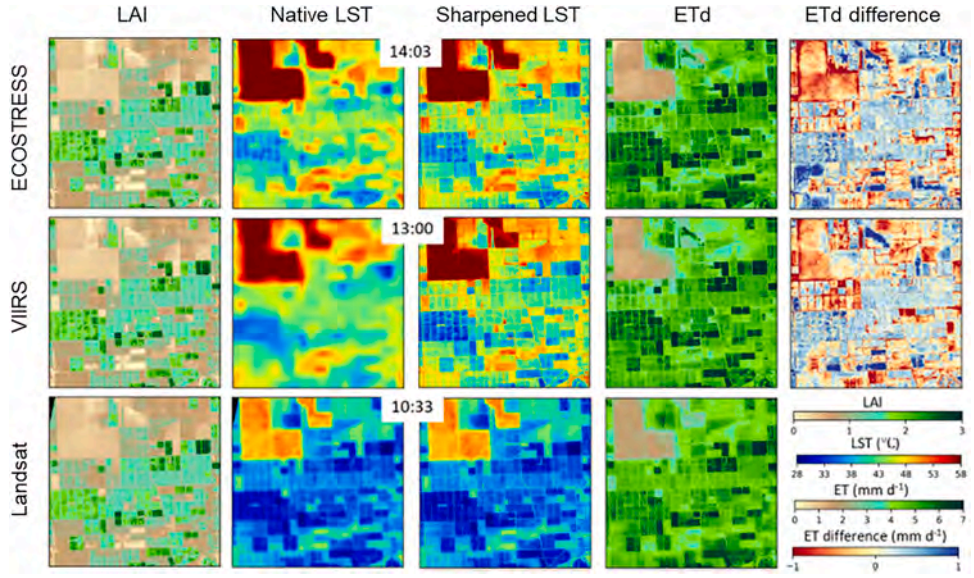

Fig. 4. Maps of LAI (first column), LST at native resolution (second column), sharpened LST (third column), and daily ET retrievals (fourth column) from DisALEXI applied to ECOSTRESS (top row), VIIRS I5 band (middle row), and Landsat (bottom row) LST sharpened to 30 m using surface reflectances from HLS over a region in the CA Central Valley. ET difference maps (ECOSTRESS (VIIRS) minus Landsat) are shown in the top (middle) panel of the fifth column. The acquisition time of the LST data is also listed. (Adapted from Xue et al., 2022).

Thermal Radiometer Experiment on Space Station (ECOSTRESS), or the Visible Infrared Imaging Radiometer Suite (VIIRS) I5 thermal band) and in planning or development (e.g., the Surface Biology-Geology (SBG), Trishna, and Land Surface Temperature Monitoring (LSTM) missions). While there is coordination between space agencies to improve harmonization of future thermal missions, each of these platforms collects data at slightly different spatial resolutions, and the TIR images are not directly interoperable (Table 2; Fig. 4). Even the thermal data collected by the Landsat series itself vary in resolution from 60 to 120 m (L7-L5).

The first step in thermal harmonization is to bring these data sources to a common resolution via sharpening (spatial downscaling), typically achieved using relationships with SR bands.

The Data Mining Sharpener (DMS) method (Gao et al., 2012) enhances spatial details in TIR or LST maps using information from the SR bands, which are usually imaged at finer resolution. DMS establishes a non-linear relationship between LST and SR bands at a coarse spatial resolution through data mining (or machine learning), then predicts LST at finer resolutions using the original SR data at their native resolution. Residuals between observed and predicted LST values are interpolated and redistributed through an energy conservation step, ensuring that the sharpened image will reaggregate to the observed image at some spatial scale. In the DMS implementation, a global model of LST and SR learned from the entire image and local models trained on smaller subsets of the image are combined based on their accuracies. Gao et al. (2012) tested the DMS using multiple SR bands over various landscapes and found it to be superior to the original TSEB thermal sharpening technique using NDVI alone (e.g., Kustas et al., 2003; Agam et al., 2007).

Xue et al. (2020) describe spatial harmonization to 30-m resolution of sub-km-resolution TIR data sources including Landsat (60–120 m), ECOSTRESS (nominally 70 m), and VIIRS I5 band (375 m) – all sharpened using 30-m SR data from HLS (Fig. 4). They describe modifications to the original DMS required in cases where TIR and SR data are collected on different platforms, including relaxation of scale of energy conservation (aggregation scale at which the sharpened image is required to match the unsharpened image) to accommodate potential errors in relative registration between the two sets of input imagery. They also note the importance of using TIR and SR data collected on the same (or very proximal) date in DMS. Any time displacement between these inputs may add noise to the sharpening process relating to surface changes in the interim (e.g., vegetation growth/senescence, harvest, rainfall/irrigation, etc.). Their study provides the basis for developing an operational thermal sharpening prototype to routinely generate high-frequency 30-m TIR data based on multi-source data.

5.2. Data fusion

Given multi-source spatially harmonized LST data layers, Challenge 6 poses the question of effective temporal interpolation between ETd retrieved at clear pixels within these layers. With sufficient sampling, a scaling flux like reference ET or insolation may suffice; however, experience has shown that this approach can result in severe artifacts during cloudy seasons when the scaling flux ratio changes significantly between clear-sky image collects. Alternatively, since ALEXI disaggregation enables development of consistent ET timeseries at multiple scales, we can use actual ET at coarser resolution to guide the gap-filling via data fusion.

The Spatial Temporal Adaptive Reflectance Fusion Model (STARFM) developed by Gao et al. (2006) combines finely detailed yet infrequent images with coarser yet more frequently available images, resulting in time series images with high spatial and temporal resolution. The approach uses the information acquired from one or two pairs of images—each comprising fine-resolution and coarse-resolution images acquired on the same date. Subsequently, this information is used to predict fine-resolution images on a different date using the available coarse-resolution image on that day. The embedded weighting strategy in STARFM considers temporal, spectral, and spatial similarities existing between the fine-resolution and coarse-resolution images. This consideration effectively transfers changes from the pair dates to the prediction dates at fine resolution. Initially tested with surface reflectance and vegetation indices, STARFM subsequently demonstrated success in the fusion of ET timeseries from Landsat and MODIS to create daily 30-m ET datasets over agricultural and forested settings (Cammalleri et al., 2013; C. 2014a; Semmens et al., 2016; Sun et al., 2017; Yang et al., 2017a; 2017b, 2018).

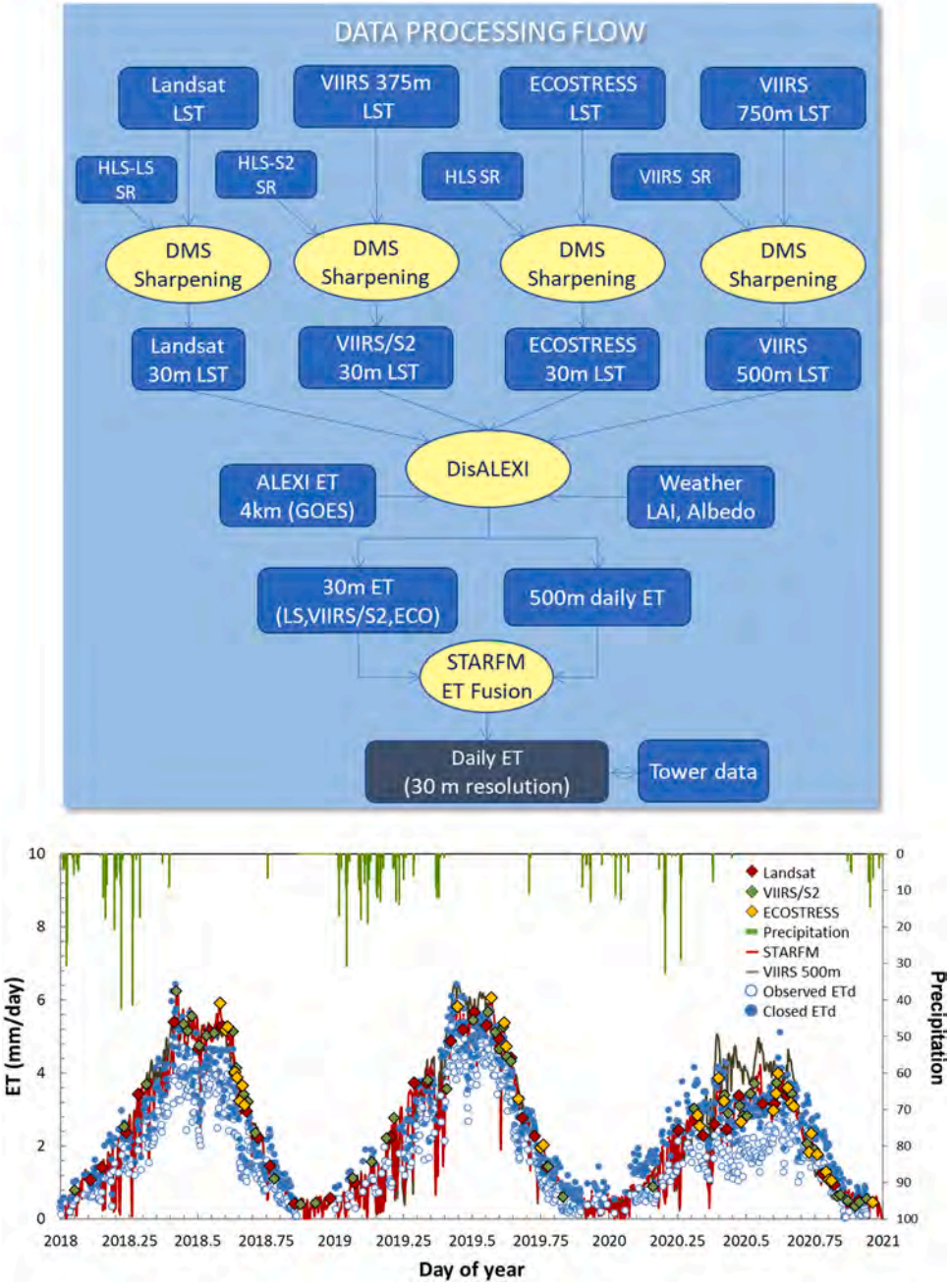

Fig. 5. Top: Schematic diagram illustrating the workflow for the multi-source ET data fusion system. Bottom: Time series comparison between measured and modeled daily ET obtained from multi-source data fusion at a GRAPEX vineyard flux site in the California Central Valley. (Adapted from J. Xue et al., 2022).

Even with data fusion, in some cases Landsat alone is not sufficient to anchor the temporal sampling at high resolution, and important features in the seasonal water use curve can be missed. Anderson et al. (2021) and Xue et al. (2021, 2022) tested augmentation of STARFM data fusion using multisource ET data generated with DisALEXI applied to Landsat, ECOSTRESS, and VIIRS I5 band TIR imagery, all sharpened to 30 m. In general, they found good consistency between the multi-source ET retrievals, given limits on view angle and time of acquisition (Fig. 5). The improved temporal sampling from the combined Landsat-like TIR sensors was beneficial during periods of persistent cloudiness and rapid surface changes. Still, Landsat outperformed ECOSTRESS and VIIRS I5 in terms of agreement with tower fluxes. This is likely due to 1) the higher native resolution of the Landsat TIR imagery, and 2) simultaneity and better co-registration of Landsat SR and TIR inputs to both DMS and DisALEXI. These are important considerations for future ET mapping missions.

6. Research and applications using TSEB

6.1. Drought and drought impacts

ET is an important measure of vegetation health that links the carbon, energy, and water cycles in terrestrial ecosystems. In the absence of other stressors such as disease, the amount of water transpired by vegetation is controlled by the biophysical properties of the plant species, how much soil moisture is available to the plants, and atmospheric factors that determine the atmospheric evaporative demand experienced by the vegetation. If root zone soil moisture is non-limiting and the plants are able to transport sufficient water to meet the atmospheric demand, they will generally maintain transpiration; however, once soil moisture falls below a certain threshold, plants will limit water usage by closing their stomata. This transition to a moisture-limited regime will lead to a decrease in ET and evaporative cooling and the appearance of moisture stress in vegetation as evidenced by enhanced canopy temperatures (Moran 2003).

Thermal-based ET models like TSEB/ALEXI/DisALEXI are well-suited for capturing these early signals of stress onset. The Evaporative Stress Index (ESI) depicts standardized anomalies in the reference ET fraction (F_{RET}: the ratio of the actual to reference ET) relative to a baseline period, using actual ET estimates from ALEXI (Anderson et al., 2007a, 2011, 2013). Normalization by reference ET serves to reduce sensitivity of ESI to atmospheric drivers of actual ET (which are well captured by the Evaporative Demand Drought Index; EDDI; Hobbins et al., 2016), focusing ESI on plant and soil moisture drivers of ET. While EDDI highlights the potential for drought development, ESI reveals drought impacts actualized on the ground.

Several studies in the U.S. and internationally have established ESI as an effective monitor of drought-induced vegetation stress (Anderson et al., 2015; Otkin et al. 2016, 2019) and soil moisture anomalies (Hain et al., 2009, 2011; Otkin et al., 2018c; Walker 2023). ESI closely tracks spatiotemporal patterns in crop and topsoil moisture conditions collected at the county scale by observers reporting to the National Agricultural Statistics Service (NASS), a valuable "ground-truth" geospatial dataset recording agricultural drought impacts (Fig. 6). In particular, the ESI has proved to be a valuable tool for tracking the onset and evolution of flash drought events, which are characterized by rapid intensification over multi-week periods (Otkin et al., 2018b, 2022). Relative to many other optical vegetation indices, the ESI often provides early warning of incipient flash drought conditions because an increase in LST due to reduced ET often occurs before visible degradation in the vegetation canopy (e.g., Anderson et al., 2013; Fig. 6). Otkin et al. (2013, 2016, 2019) showed that rapid decreases in the ESI occurred during notable flash drought events across the U.S.. The ESI-based rapid change index (RCI) depicts time-accumulated moisture stress change, with larger RCI values associated with an increased risk for drought development over subsequent weeks (Otkin et al., 2014, 2015a). These tools have been presented at focus group meetings with farmers and ranchers, with survey feedback indicating good utility for tracking on-the-ground conditions (Otkin et al., 2015b, 2018a; Haigh et al., 2019).

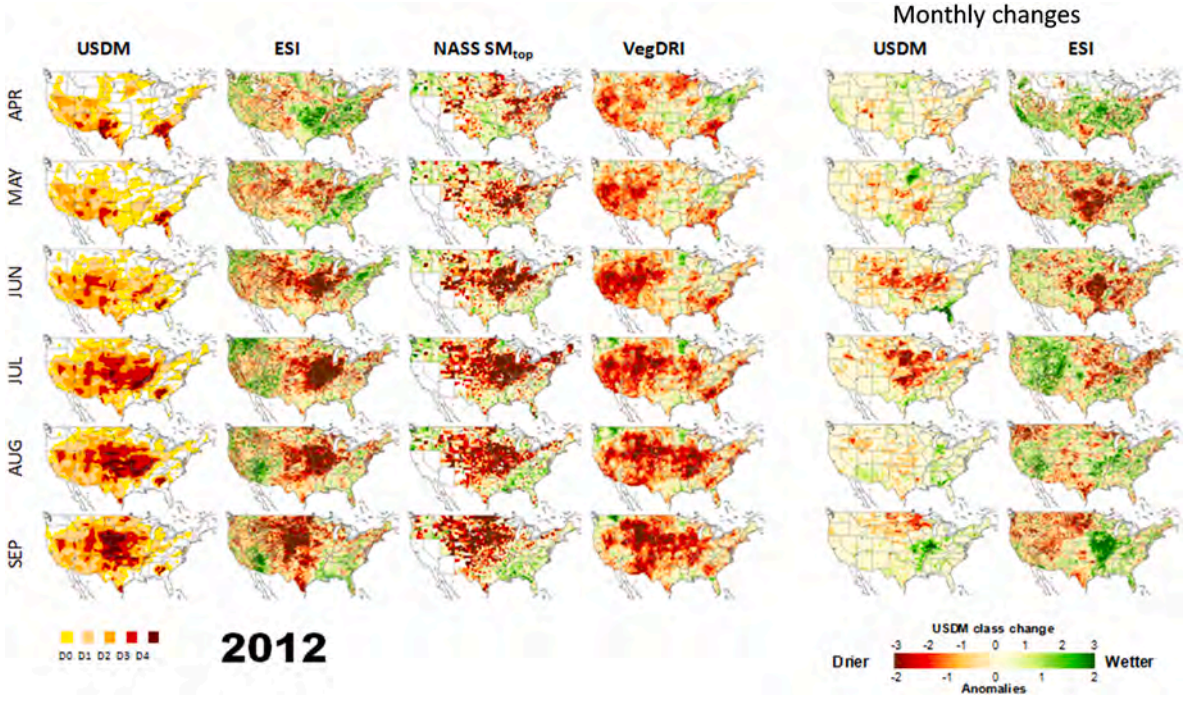

Fig. 6. Left four columns: Monthly maps of U.S. Drought Monitor (USDM) drought class, Evaporative Stress Index (ESI), and standardized anomalies in National Agricultural Statistics Service (NASS) county-level records of topsoil moisture condition and the NDVI-based Vegetation Drought Response Index (VegDRI) for April-September 2012. Right columns show change in USDM class and ESI between monthly reports, expressed as normalized anomalies. (Adapted from Anderson et al., 2013).

As an integrative indicator of crop health, reflecting both crop condition and soil moisture status, ESI can be a useful predictor of crop yields and a warning of reductions in productivity due to water stress. ESI at 4–10 km from ALEXI has been shown to correlate well with crop yields in the U.S. (Mladenova et al., 2017), Brazil (Anderson et al., 2016b), and the Czech Republic (Anderson et al., 2016a; Jurečka et al., 2021). More recently, Yang et al. (2018, 2021a) examined yield relationships with ESI developed at 30-m using fused Landsat-MODIS ET timeseries over sites in the U.S. Corn Belt. They demonstrated value in resolving vegetation stress at the field scale, effectively unmixing signals from multiple landcovers (different crops, forest, riparian vegetation, etc.) that can jointly contribute to a blurred moisture response at the ALEXI pixel scale. For corn crops, correlations between 30-m ESI and yield peaked at around tasseling, a stage of high sensitivity to soil moisture deficiencies.

DisALEXI ESI at 30-m resolution has also been used to study impacts of drought stress on forested lands, down to scales approaching that of individual tree crowns. In a managed pine plantation in North Carolina, Yang et al. (2020) found higher impact of drought on water use and tree growth rate in young pine stands than in more mature stands. The generally mild impact of drought on stand water use observed in this case might relate to the relatively shallow groundwater, which can mitigate the drought impacts on older trees with deeper root systems. In contrast, over a temperate forest with thin soil layers in Missouri, Yang et al. (2021b) found stronger impact of drought on forests expressed in the dynamics of fused DisALEXI 30-m F_{RET} timeseries (Fig. 7). In this study area, ESI showed good temporal agreement with pre-dawn leaf water potential measurements, particularly during drought years. Yang et al., demonstrated a close a relationship between forest water use and tree die-off after drought years, optimized when the F_{RET} anomaly was averaged over the two years prior to the mortality event. This suggests that the condition of the forest before the drought influenced tree mortality, as well as the stress experienced during the drought itself.

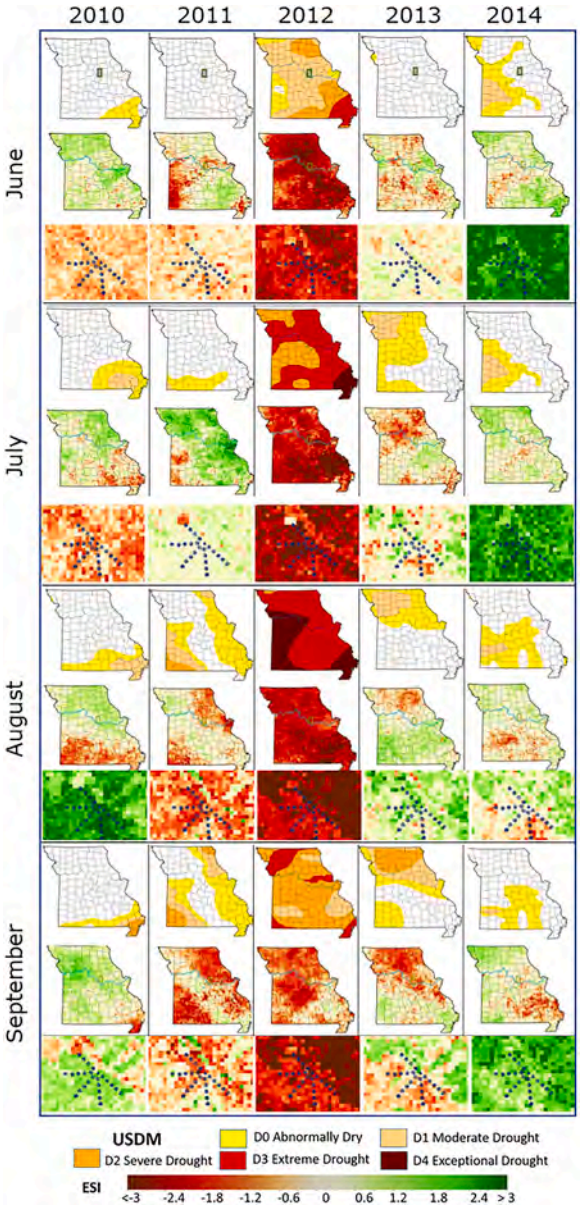

Fig. 7. USDM and multi-scale ESI at 4-km and 30-m over the MOFLUX experiment site in Missouri (location indicated in the top row). The dots represent transects along which tree mortality was recorded on the ground (Adapted from Yang et al., 2021b).

6.2. *Water use monitoring and management*

6.2.1. *Vineyards and orchards*

The ability to estimate water use at field scale without a priori knowledge of additional (non-rain-sourced) water applied makes TIR-derived ET a valuable asset for water management over irrigated landscapes (Anderson et al., 2012). In the case of the TSEB, this is especially relevant for highly structured crops where bare soil exposure contributes significantly to the energy budget and composite radiometric temperature signal, necessitating a two-source modeling scheme.

Evaluating and improving the TSEB for irrigation management in structured canopies was a major focus of the Grape Remote sensing Atmospheric Profile and Evapotranspiration eXperiment (GRAPEX) conducted in California vineyards, a partnership involving E & J Gallo, the USDA, and multiple federal agencies and academic institutions (Kustas et al., 2018). In California, vineyards require specialized irrigation management due to the use of deficit irrigation for improved grape quality, exacerbated water scarcity from ongoing droughts, and complex trellis designs that hinder straightforward satellite monitoring. Three key questions were posed by E & J Gallo partners: 1) when is the optimal spring start date for irrigation?; 2) what is the weekly water volume needed to achieve target stress levels?; and 3) can the model differentiate total ET between vines and cover crops? The perception is that maximum water savings lies in delaying irrigation while the soils dry out from springtime rains, and thereafter applying only the water needed to achieve the target vine stress levels.

The GRAPEX project officially started in 2013 with the installation of eddy covariance flux towers in two vineyards in San Joaquin County, California (SLM in Fig. 8). To better capture the range in California viticultural practices, trellis designs, and climate conditions, the GRAPEX project strategically expanded in 2017 to include vineyards in Sonoma and Madera Counties (Fig. 8; BAR and RIP, respectively). Knipper et al. (2020) conducted a multi-year evaluation of DisALEXI daily ET across these collective sites and reported an RMSE value of 0.9 mm d^{-1}. In 2018, a synthetic stress test was conducted in a Variable Rate Drip Irrigation (VRDI) equipped vineyard by withholding irrigation to induce short-term and differential stress across the block. Knipper et al. (2019) demonstrated that fused Landsat-MODIS DisALEXI timeseries were able to detect the induced stress, while "business-as-usual" monitoring techniques using only NDVI were not. Since 2018, the DisALEXI system has provided near-real-time daily ET estimates for various vineyards. These estimates are integrated into a weekly irrigation dashboard for growers and into the Vineyard Irrigation Data Assimilation (VIDA) model to determine rootzone soil moisture at 30-m resolution (Lei et al., 2020; Chen et al., 2022).

Inspired by the success of GRAPEX, USDA ARS initiated the Tree crop Remote sensing of Evapotranspiration eXperiment (T-REX) in 2021 (Bambach et al., 2024), partnering with the Almond Board of California, Olam Food Ingredients, and other institutions. Similar to GRAPEX,

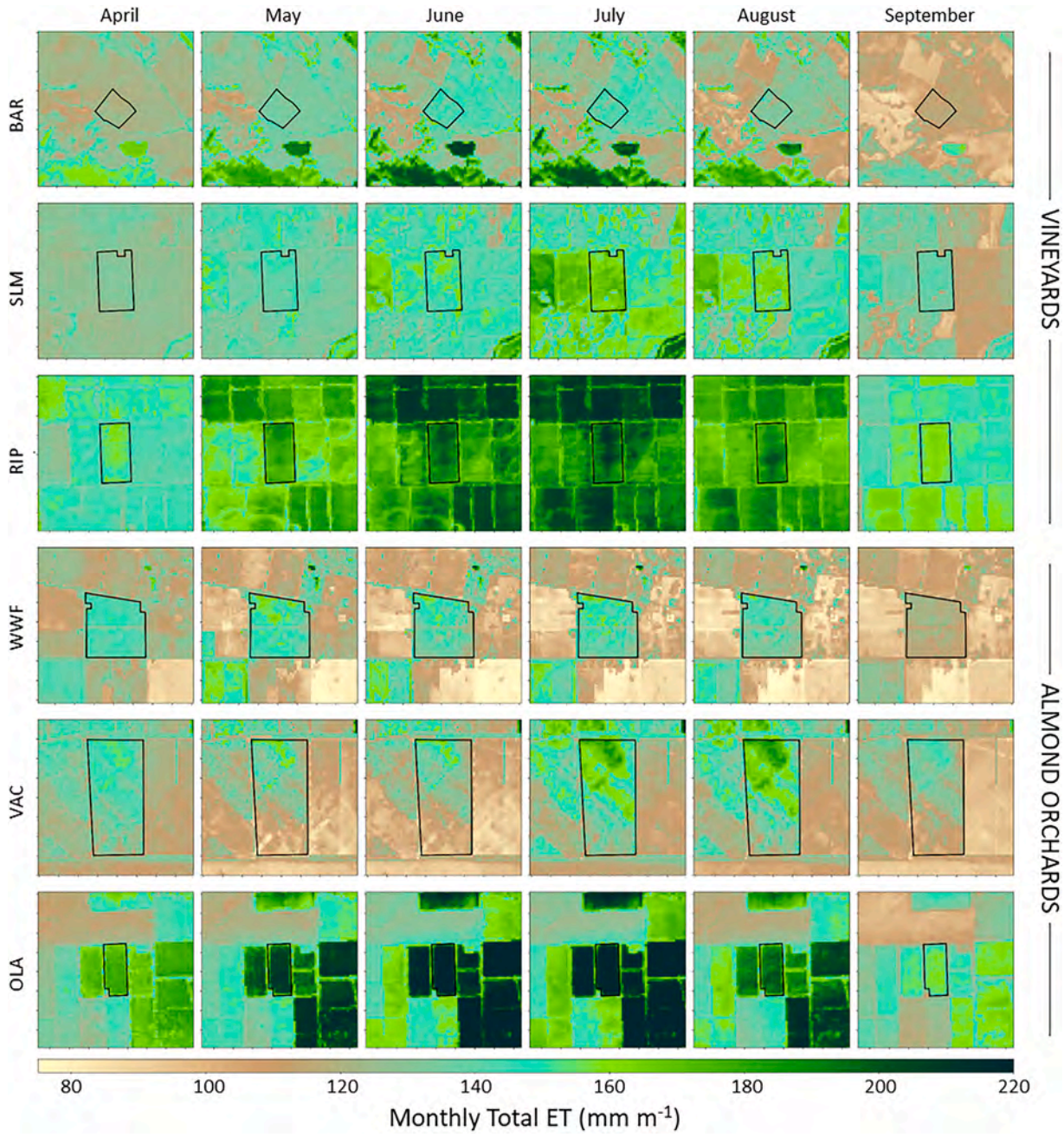

Fig. 8. Maps of 30-m monthly ET (April – September, 2022) over GRAPEX and T-REX intensive study sites (outlined in black).

T-REX focuses on optimizing water use and carbon sequestration in California's perennial tree crops. An initial evaluation by Bambach et al. (2023) reported mean absolute errors (MAE) of 0.8 to 1.1 mm d^{-1} for fused, 30-m daily ET in comparison with flux observations in T-REX almond orchards in Solano, Yolo, and Madera Counties, CA (VAC, WWF, and OLA sites, respectively; Fig. 8). In 2023, T-REX expanded its scope to include a regenerative almond orchard and four olive orchards, supported by California Olive Ranch.

The GRAPEX/T-REX projects provided a unique opportunity to extend the TSEB model to data from uncrewed aerial vehicles (UAVs, also called drones) towards precision agriculture activities. The AggieAir UAV Program at Utah State University (https://uwrl.usu.edu/aggieair/) participated in these experiments since 2014, using both vertical take-off and landing (VTOL) and fixed wing aircrafts (Fig. 9). These systems provide high-resolution (cm-scale) imagery in multiple spectral bands (blue, green, red, near infrared, TIR) as well as a description of the canopy geometry (height, area, volume) from the UAV-derived digital surface model and point cloud. At these fine scales, canopy and soil temperatures can be measured directly, enabling a version of the TSEB (TSEB-2T; Nieto et al., 2019) that does not require initial assumptions about potential canopy transpiration (e.g., via PT or PM approximations; Eq. (9)). The spatial detail and canopy structure information from the UAVs also facilitate investigation of the impacts of shadowing on surface temperature and surface reflectance retrievals at the Landsat pixel scale (30 m or larger), which can be significant in vineyard and orchard systems and dependent on time of image acquisition and row direction (Aboutalebi et al., 2019) (Fig. 9).

Implementations of TSEB models in vineyards and orchards have also been conducted outside of the U.S. using UAV and satellite imagery (Minacapilli et al., 2009; Cammalleri et al., 2010; Andreu et al., 2015; Corbari et al., 2015).

Fig. 9. Top row: Examples of the USU AggieAir drone technology used in the GRAPEX and T-REX projects, including (left) a custom hybrid fixed-wing drone with 1.5+ hour flying capabilities, and (right) vertical take-off and landing (VTOL) drone for surveying smaller areas. Bottom row: Example of the canopy structure in vineyards (left) and almonds (right) that UAV imagery can describe. Note the interrow conditions (with or without cover crop), tall, clumped canopy of the main crop, and the changes in interrow exposure to sunlight depending on sun angle and row direction.

6.2.2. *Forest management*

Ecosystem services in provisioning water are an important consideration in the management of forested systems, and remotely sensed ET can provide historical and spatially explicit information on the impacts of different management activities on forest water yield. Over the managed pine plantation in North Carolina mentioned in Section 6.1, Yang et al. (2020) analyzed stand recovery after thinning and found a clearer trend in water use change than in NDVI change. Related work was conducted in the New Jersey Pinelands, quantifying rates of ET recovery after thinning and seed tree harvest and the variable impacts of prescribed burning on ET relating to fire severity (Isaacson et al., 2023). Comparisons with flux tower observations from the US-Slt Ameriflux site yielded MAE of 0.8 mm d^{-1}. The ET fusion system provided adequate spatial and temporal resolution to capture changes in water use at the scale of management, suggesting these data have value in predicting watershed water yield response under different forest management scenarios.

6.3. *Data assimilation and model diagnostic applications*

In contrast to ALEXI/TSEB, prognostic land surface models (LSMs) neglect satellite-based LST retrievals and instead solve the surface water and energy balance using meteorological forcing data and a bottom-up parameterization of the relationship between land surface states (e.g., soil moisture and temperature) and surface water/energy fluxes (e.g., ET, infiltration, and recharge). Critically, ALEXI/TSEB and LSMs provide a partially overlapping set of outputs (e.g., ET) while relying on fundamentally different approaches for capturing the impact of water-stress on surface fluxes. In place of LST, LSMs require accurate measurement (or forecasting) of precipitation to track temporal soil moisture variations and detect the onset of water stress.

This mutual independence opens several opportunities. For example, due to their fundamentally different approaches for solving the surface energy balance, energy flux errors in prognostic LSMs are typically independent of comparable ALEXI/TSEB errors (Crow et al., 2005). Such independence provides the theoretical basis for the assimilation of ALEXI/TSEB energy flux products, or related soil moisture proxies like ESI, into prognostic LSMs. This assimilation can occur either in isolation or in tandem with microwave-based soil moisture products. For example, studies have examined the joint assimilation of microwave and ESI-based soil moisture estimates into the LSM portion of a numerical weather prediction system (Hain et al. 2011, 2012; Mishra et al., 2021), identifying added value relative to a baseline case of assimilating only microwave-based soil moisture retrievals. One key reason is the increased vertical support of root-zone ALEXI ESI assessments versus the superficial support (i.e., top 5 cm only) of microwave soil moisture retrievals. A similar joint assimilation strategy is currently being applied for the operational monitoring of root-zone soil moisture within irrigated vineyards and orchards – see discussion of the VIDA system in Section 6.2.

Land data assimilation only targets purely random error present in a prognostic LSM. In reality, LSM errors are often systematic in nature (i.e., statistically related to land surface states), commonly arising from the poor parameterization, or outright neglect, of certain land processes. A growing body of literature has demonstrated the value of ALEXI/TSEB products for diagnosing such errors. For example, Hain et al. (2015) utilized ALEXI ET estimates to explicitly map areas where a LSM neglects the impact of tile drainage, irrigation, and surface/groundwater coupling on surface energy balance modelling. A related challenge in LSMs is the accurate characterization of available soil water storage for root uptake and transpiration. Such storage fundamentally establishes ecosystem susceptibility to periods of low precipitation or enhanced evaporative demand – but is also sensitive to poorly mapped subsurface characteristics (e.g., maximum rooting depth and depth to bedrock). Nevertheless, studies established the potential for utilizing ALEXI/TSEB ET time series as a top-down constraint on such storage capacity (Cammalleri and Ciraolo 2012; Stocker et al., 2023).

ALEXI/TSEB energy flux estimates can also contribute to an improved understanding of water storage versus flux relationships. For example, Lei et al. (2018) highlighted the ability of ALEXI ET estimates to detect systematic bias in LSM parameterizations of ET versus soil moisture coupling strength. Left uncorrected, such bias can degrade the accuracy of land-model ET estimates (Dong et al., 2020, 2022) and, therefore, short-term numerical weather forecasts dependent on such

estimates (Crow et al., 2020). More recent work in Koster et al. (2024) has extended this ability to the characterization of non-linear regime transitions in the relationship between soil moisture and ET.

7. Regional to global scale implementations

To support the broad spectrum of research and applications discussed in Section 6, the multi-scale family of TSEB models has been implemented in several operational and on-demand systems operating from field to global scales. Some of these systems are described below.

7.1. GET-D (NOAA)

The NOAA-NESDIS Geostationary Evapotranspiration and Drought (GET-D) product system was developed to operationally generate and distribute ALEXI ET and ESI datasets over the GOES domain. Starting in September 2016, GET-D commenced operational runs at NESDIS Office of Satellite and Product Operation (OSPO), posting products to the NOAA-STAR Drought Monitoring Web Site: https://www.star.nesdis.noaa.gov/smcd/emb/droughtMon/products_droughtMon.php. At that time, the operational GET-D product system used GOES-13/15 imager data to generate daily ET and ESI at 8-km resolution over a North American domain for the years from 2001 to 2017 (Fig. 10, left). These products were upgraded to 2-km resolution over CONUS in 2018 (Fig. 10, right), when the NOAA primary operational geostationary satellites switched to GOES-16/17, carrying the Advanced Baseline Imager (ABI). In 2023, the GOES-18 satellite replaced GOES-17 as GOES-West, with improvements to the ABI thermal sensors. Detailed information regarding the science and software architecture of the upgraded GET-D product system can be found in Fang et al. (2019, 2022). Currently the daily ET data products are routinely distributed to Environmental Modeling Center of NOAA National Weather Service (NWS) for numerical weather product model verification/validation. The CONUS ESI data product is distributed to the National Integrated Drought Information System (NIDIS) as a reference for U.S. Drought Monitor publication.

7.2. SERVIR (NASA) – global ALEXI

Global near-realtime (NRT) applications of the classic version of ALEXI would require harmonized LST data from the global geostationary datasets, which is not yet available in NRT and cannot provide LST observations at high latitudes ($> 60°$). To facilitate routine global execution of ALEXI, a polar-orbiter-based (e.g., AVHRR, MODIS, VIIRS) proxy for the morning LST rise has been developed using a data-mining approach based on day-night observations of LST and other geophysical variables (Hain and Anderson 2017). This approach uses a rule-based regression tree algorithm (RuleQuest, Cubist) to compute a set of rules linking the predictor variables with the geostationary-observed DT_R (e.g., GOES) training data. The following predictor variables were shown to exhibit the strongest relationships with the training data: (1) MODIS day-night LST difference, (2) MODIS day LST, (3) MODIS night LST, (4) leaf area index, and (5) topographic variability. Currently, estimates of the morning LST rise are used in a NRT global ALEXI framework at 0.05-° spatial resolution using a long-term satellite time series from MODIS and VIIRS, run at NASA's Short-Term Prediction Research and Transition Center (SPoRT; https://weather.ndc.nasa.gov/sport/). The modeling framework also provides a NRT global ESI product hosted and routinely available from NASA's SERVIR project (https://servirglobal.net/Global/Evaporative-Stress-Index). These global data are being ingested into the Geoglam Crop Monitor (https:/cropmonitor.org), the USDA Foreign Agricultural Service's Global Agricultural & Disaster Assessment System (GADAS), and NASA's DISASTERS Dashboard (https://disasters-nasa.hub.arcgis.com/; Fig. 11). An excerpt of the global ESI product over CONUS is distributed by the National Integrated Drought Information System (NIDIS; https://www.drought.gov/data-maps-tools/evaporative-stress-index-esi), over North America by Agri-Food Canada (https://agriculture.canada.ca/en/agricultural-production/weather/evaporative-stress-index), and over Central Europe by Intersucho (https://www.intersucho.cz/en) (Trnka et al., 2020).

7.3. OpenET

The OpenET framework (https://etdata.org; Fig. 12) on Google Earth Engine (GEE) was released to the public in 2021 with the goal of delivering open and objective field-scale (30-m resolution) ET data in support of water management and decision making (Melton et al., 2022). OpenET is a collaborative effort involving scientists from multiple federal agencies, academic institutions, and non-profit organizations. Importantly, a broad range of stakeholders has been engaged since early in the platform design process to ensure that the system delivers

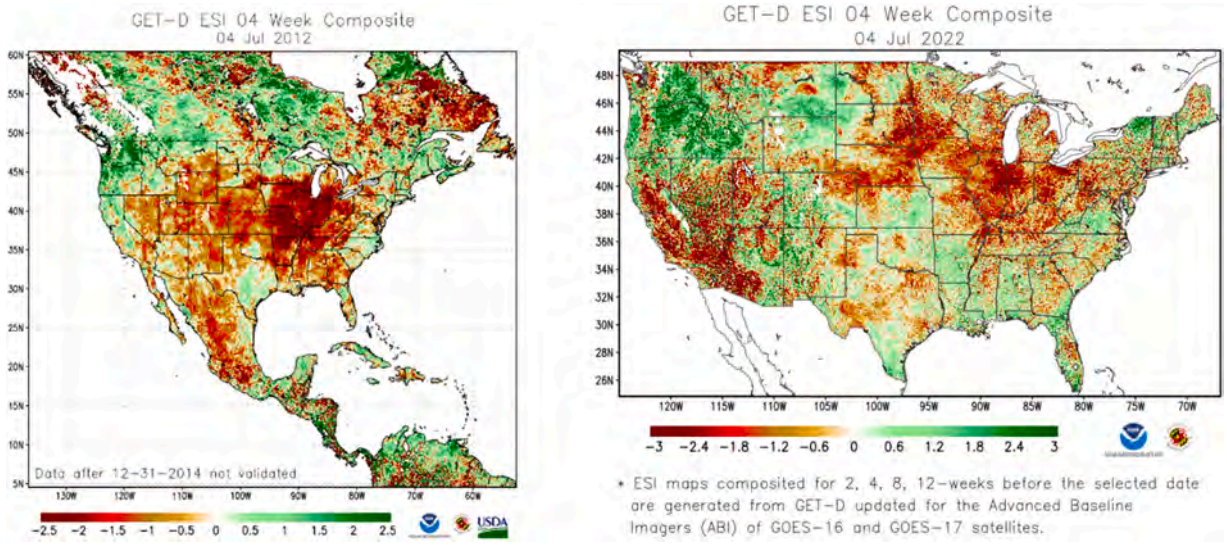

Fig. 10. GET-D ESI products (4-week composite) for July 4, 2012 based on GOES13/15 (8-km resolution) over the North America domain (left) and for July 4, 2022 using GOES16/17 (2-km) over the CONUS domain (right).

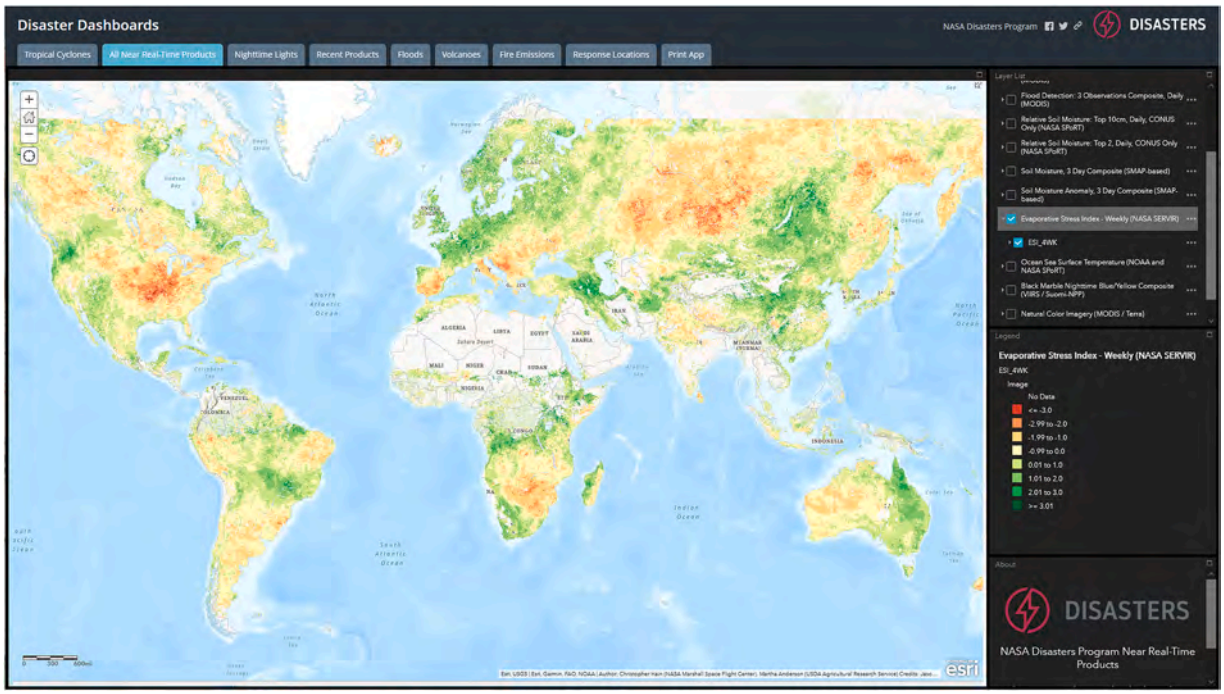

Fig. 11. Global ESI at 5-km resolution (4-wk composite for July 2012) developed by NASA-SPoRT and distributed through the NASA DISASTERS mapping portal.

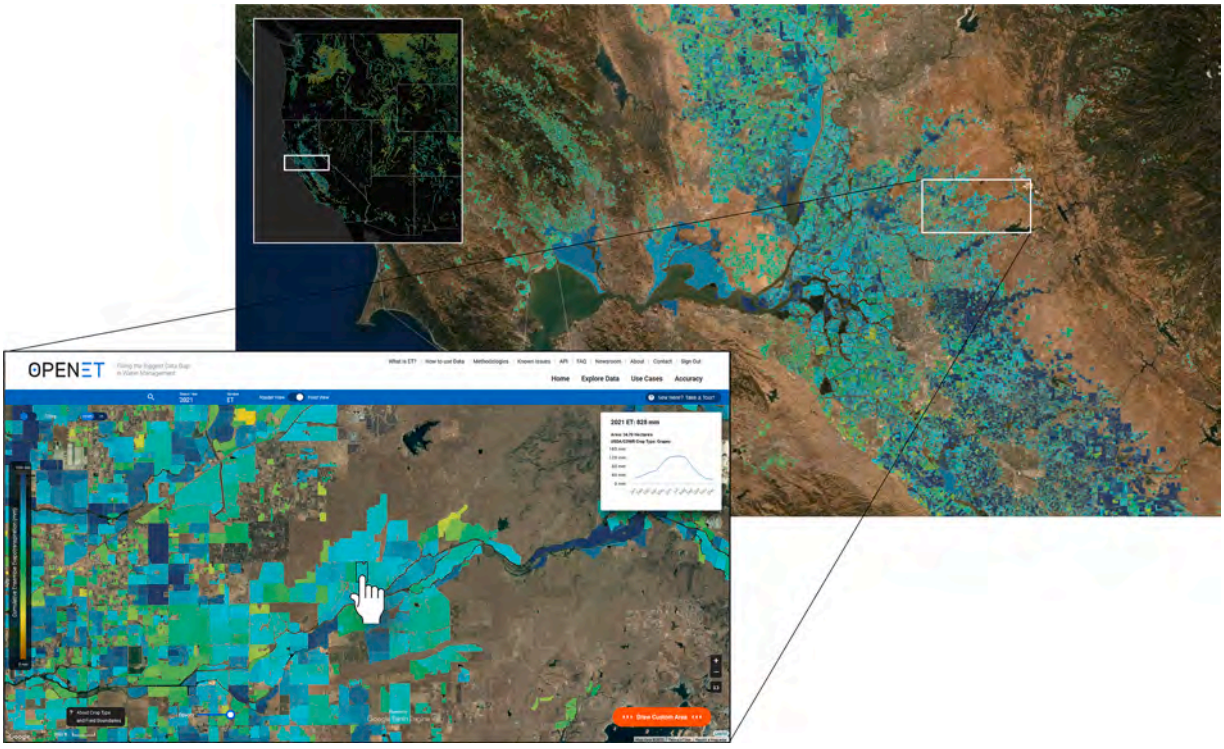

Fig. 12. Map of ensemble ET for 2021 over the SLM GRAPEX intensive site from the OpenET web user interface (https://etdata.org).

useful information in a usable and transparent way. These include representatives from local, state, federal and tribal government water management agencies, small family farms, and large agricultural organizations.

OpenET has taken an ensemble modeling approach to data generation, using six well-established ET remote sensing models, including DisALEXI, that have been ported to GEE. These models represent a diversity of modeling approaches, with different key inputs, different assumptions and sensitivities – some using TIR inputs, and others more sensitive to surface reflectance and vegetation indices. Evaluation in comparison with eddy covariance measurements from over 150 flux towers in the U.S. demonstrated that on average over all crop types (rainfed and irrigated), the ensemble average ET performs better than any individual model (Volk et al., 2024). For example, at the monthly timestep, mean absolute error (MAE) for croplands from individual models ranges from 0.60 to 0.76 mm d^{-1} (with DisALEXI at 0.66 mm

d^{-1}), while the ensemble MAE was 0.53 mm d^{-1}. Largest MAE for DisALEXI/ensemble members were observed in evergreen forest (MAE=0.97/0.84–1.04 mm d^{-1}) and wetland/riparian (MAE=1.05/0.72—1.06 mm d^{-1}) land covers, both with positive ET bias in all models. Further adjustment of the initial value of α_{PTC} for conifers may be warranted; and with accurate land-cover information at the 30-m scale, DisALEXI flux estimates for wetlands may be improved by increasing the heat storage term ratio (see Section 4.2).

The GEE implementation of DisALEXI (Yang et al., 2022) is being leveraged to extend ET mapping applications in GRAPEX/T-REX over the full California Central Valley agricultural region, effectively bringing the model to the satellite data and leveraging the cloud computing resources available on GEE. In the intercomparison study of Volk et al. (2024), DisALEXI outperformed all other models over vineyard sites including the ensemble, yielding an MAE of 0.43 mm d^{-1}. The OpenET platform also facilitates intercomparison between different Landsat-scale ET retrieval approaches, allowing investigations of the unique value of TIR imaging in terms of sensitivity to moisture stress and water use over the full cycle of crop development. Notably, with TIR we see greater sensitivity to deficit irrigation and to water applied during periods with low cover, e.g., at the beginning of the season or between double cropping cycles when irrigation is often applied to flush salts

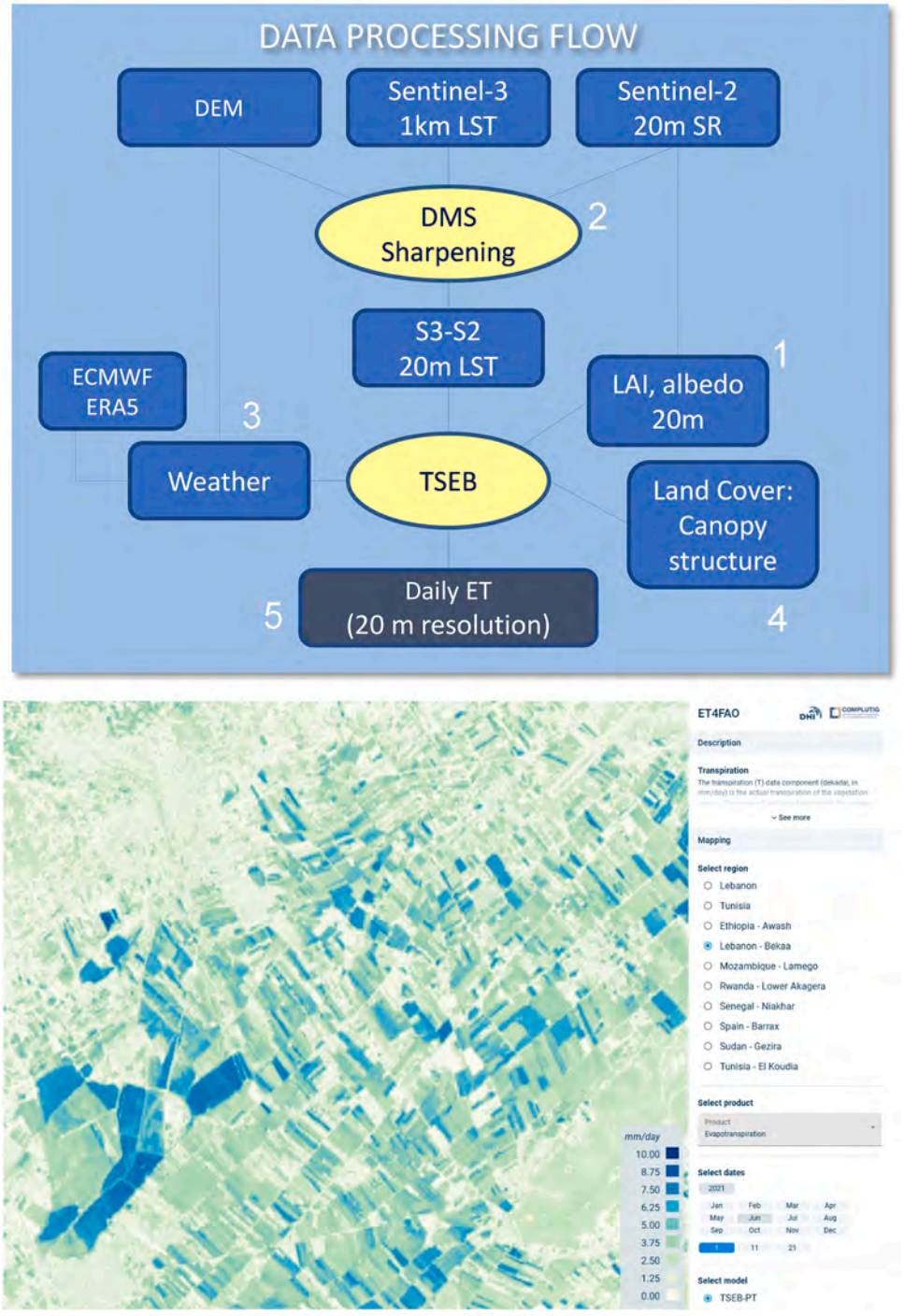

Fig. 13. Top: Workflow for Sen-ET (numbers correspond to modeling components tabulated in the text). Bottom: Map of 20 m ET obtained using the Sen-ET approach in the Bekaa Valley in Lebanon, taken from the ET4FAO portal (https://et4fao.dhigroup.com/).

from the soil profile. The latter can be missed by OpenET models based primarily on surface reflectances.

Initial coverage in OpenET is limited to the western United States, but with continued interest and support, plans are to expand to full U.S. and then global coverage. The data can be accessed through a web-based interface, or through an automated programming interface (API) for direct ingestion into existing management toolkits.

7.4. SEN-ET (Copernicus)

Another recent development for the TSEB family was the implementation of TSEB within the Sen-ET toolkit (https://www.esa-sen4et.org/) using data provided by the European Union's Copernicus Earth Observation program. Copernicus consists of a space component, including the Sentinel satellites and other contributing missions, and downstream services such as Copernicus Climate Change Service (C3S). Of most relevance for ET modeling are the Sentinel-2 and −3 satellites. Sentinel-2 provides multispectral shortwave observations with spatial resolution of 10 – 60 m and revisit period of 5 days with two satellites operating in tandem (Drusch et al., 2012). Sentinel-3 adds observational capabilities in the TIR wavebands, acquired at around 1-km resolution with daily revisit time (Donlon et al., 2012). To improve the spatial resolution to sub-field scale (20 m), the DMS thermal sharpening tool is employed (Section5.1).

The Sen-ET approach consists of five main components (Fig. 13), each using open-access data and implemented as open-source code:

1. Modelling of surface biophysical properties with 20-m resolution using Sentinel-2 observations and SNAP toolbox (https://step.esa.int/main/) and Python scripts (https://github.com/hectornieto/pypro4sail);
2. Sentinel-3 and −2 thermal-shortwave data fusion using a Python implementation of DMS (https://github.com/radosuav/pyDMS), which produces daily 20-m LST;
3. Surface meteorological reanalysis from ERA5 model provided by C3S and corrected for topographical effects using Copernicus Digital Elevation Model (DEM) and Python scripts (https://github.com/hectornieto/meteo_utils);
4. Setting of surface properties such as vegetation height using a landcover map, either produced by Copernicus Land Monitoring Service (100-m resolution) or from Sentinel observations (World-Cover – 10-m resolution);
5. Modeling of land surface fluxes at 20-m resolution using the above inputs and open-source implementation of the TSEB model (https://github.com/hectornieto/pyTSEB).

The feasibility of the Sen-ET approach was evaluated in a study in Denmark, which achieved promising results (Guzinski and Nieto 2019) and led to the implementation of the Sen-ET approach as an open-source plugin for the SNAP toolbox (https://www.esa-sen4et.org) (Guzinski et al., 2020). In this study, the approach was evaluated using EC measurements in Europe, Africa and North America while running with purely global datasets and without any site-specific parameterization and resulting in good accuracies. In a follow up study, the Sen-ET approach was demonstrated for national-extent field-scale mapping of ET in Lebanon and Tunisia for the purpose of assisting the Food and Agriculture Organization of the United Nations (FAO) with monitoring of the Sustainable Development Goal (SDG) indicator 6.4.1 – water use productivity (Fig. 13). In the same study, the daily ET (gap-filled and aggregated to decadal timestep) was evaluated against measurements in irrigated and rainfed agriculture in Spain and Tunisia resulting in a bias of 0.3 mm d^{-1} and root-mean-square error (RMSE) of <1 mm d^{-1} (Guzinski et al., 2021). Other studies using the Sen-ET approach were conducted in India (Chintala et al., 2022), Indonesia, the Italian Alps (De Santis et al. 2022; Perico et al., 2022), and Spain (Aguirre-García et al. 2021; Burchard-Levine et al., 2021).

One of the main challenges of using Sentinel-3 imagery is that LST sharpening from 1 km to 20 m causes larger bias for extreme temperatures (i.e. systematic overestimation over colder pixels while underestimating the hottest pixels), since such LST downscaling approaches are not able to describe the whole dynamic range captured at the finer resolution (Sanchez et al., 2024). To minimize this issue, the sharpening method has recently been improved by incorporating Landsat LST imagery, in particular the LST variability within each 1×1 km tile (Guzinski et al., 2023). Based on the most recent results of Guzinski et al. (2023), overall daily MAE in semi-arid rainfed and irrigated croplands was below 0.7 mm day^{-1}, but largest errors occurred in an almond orchard with MAE=0.93 mm day^{-1}. This was most likely due to uncertainties in surface roughness estimation related to the land-cover information at the 20-m scale.

The Sen-ET approach and TSEB model are currently under evaluation by the Copernicus Land Monitoring Service for operational production of a proposed global ET product (300-m spatial resolution, 10-d timestep).

8. Remaining challenges and ongoing research

8.1. Cloud-tolerant microwave-based temperature inputs

Especially at the global scale and over the tropics, we encounter limitations in LST sampling from TIR imagers like MODIS and VIIRS (Challenge 8). Extended periods without a clear-sky retrieval stretch the ability of interpolation techniques. Even in CONUS, relying solely on TIR-based LST estimates leaves us with a poor ability to pinpoint response of ET to rainfall and relief from drought, which typically coincides with cloudy conditions. To enhance our capacity to retrieve ET under all-weather conditions, cloud-tolerant microwave Ka-band observations can be leveraged to estimate LST (Holmes et al., 2009, 2016). The combination of microwave LST from multiple polar orbiting satellites allows almost daily characterization of the diurnal cycle in LST at a spatial resolution of ~25 km (Holmes et al., 2015). The utility of microwave-based LST for energy balance estimates of evaporation has been demonstrated in the context of the ALEXI framework (Holmes et al., 2018), and is currently being tested for integration withing the global SERVIR product system (Section 7.2). Not only are microwave retrievals more temporally dense, they also exhibit less day-to-day noise being more resistant to cloud contamination (Fig. 14). This significantly benefits the outlier detection, smoothing, and gap-filling procedures used in creating daily ET timeseries.

A related effort has been implemented within the GET-D system, using a regression tree machine learning technique to synergize GOES ABI thermal observations with Ka-band microwave data available from the Advanced Microwave Scanning Radiometers (AMSRs) on current Japanese GCOM-W and future GOSAT satellites. Using LST simulations/forecasts from the Climate Forecast System Reanalysis for harmonization, the machine learning technique merges GOES TIR observations with MW to derive LST under both clear-sky and cloudy conditions. Notably, the all-weather ET product significantly increased data coverage by approximately 260% over the CONUS domain in 2018 when compared to the clear-sky ET product (Fang et al. 2022). This substantial improvement in data availability is of utmost importance in promoting the application of the GET-D products.

8.2. E/T partitioning

Accurate E and T partitioning is important for understanding irrigation efficiencies and for isolating leaf and soil water status (Kustas and Anderson 2009; Kustas et al., 2019), and was recently identified as one of ten major knowledge gaps in ET research (Fisher et al., 2017). However, accurate measurements of E and T needed to test and improve partitioning in ET models have been difficult to obtain and extrapolate to field scale (Kool et al., 2014). Earlier studies of TSEB partitioning from

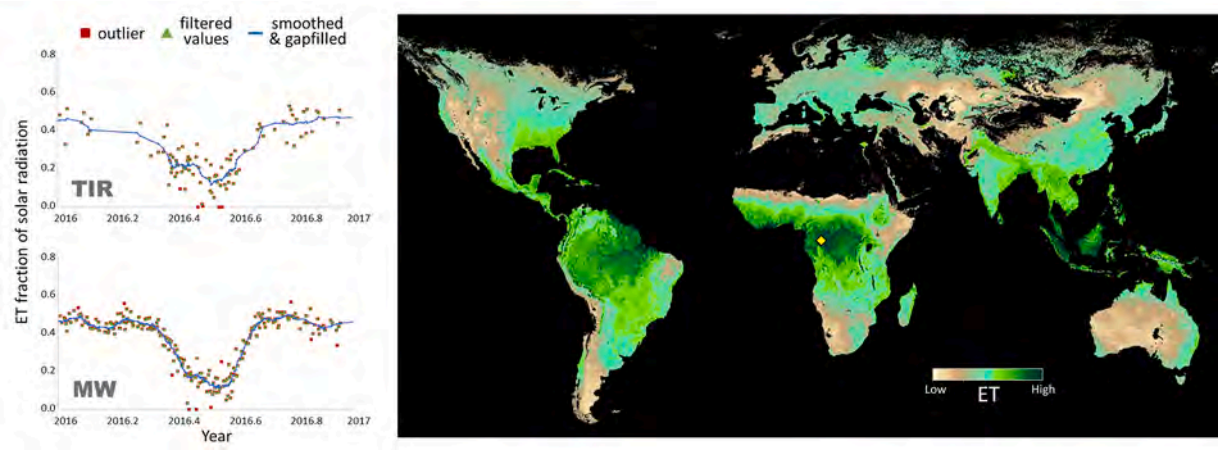

Fig. 14. Right: Global ALEXI ET map generated at 25-km resolution with microwave (MW) LST. Left: Comparison of ET/solar radiation timeseries extracted from TIR and MW versions of ALEXI at a point in the African tropics (yellow diamond). .

the Bushland Evapotranspiration and Remote Sensing Experiment of 2008 (BEAREX08; Evett et al., 2012) used sapflow and microlysimeter data to quantify observed transpiration and soil evaporation fluxes (Agam et al., 2012; Colaizzi et al. 2014); however, these measurements are very labor-intensive and accurate results are difficult to obtain. Recent advancements based on correlations between high frequency eddy covariance measurements of water vapor and CO_2 concentrations show promise (Scanlon and Sahu 2008; Scanlon and Kustas 2010, 2012; Zahn et al., 2022) but require more extensive testing.

TSEB estimation of E (LE_S) and T (LE_c) has been examined in annual row crops (Anderson et al., 2005; Colaizzi et al. 2014, 2016a; Sun et al., 2017; Peng et al., 2023), perennial crops (Burchard-Levine et al., 2022a; Nieto et al., 2022; Knipper et al., 2023; Gao et al., 2023), and forested systems (Yang et al., 2017b; Burchard-Levine et al., 2022b). The accuracy of E and T partitioning is influenced by the leaf area index value (Kang et al., 2022) applied as well as the transpiration algorithm (e.g., Colaizzi et al. 2014; Knipper et al., 2023). Particularly in arid environments with sparse vegetation, the standard soil resistance formulation used in TSEB may require modification (Li et al. 2019), and optimization of plant transpiration parameters is needed in isolated irrigated orchards/vineyards (Kool et al., 2021). Improvements in LAI retrievals from remote sensing and E and T separation have come from the use of very fine resolution UAV imagery 10^0 – 10^1 cm pixel resolutions) and machine learning tools (Gao et al., 2022; Aboutalebi et al., 2022). The partitioning of ET between Tcrop (from the main crop) and E+Tcover (from the interrow, bare soil evaporation + cover-crop transpiration) from TSEB as applied to UAV data (Fig. 15) allows for additional research on net irrigation (e.g., for only grapevine plants and almonds trees excluding interrow crop), water stress estimation from an energy balance perspective (instead of empirical relationships), and a closer examination of linked agricultural water and carbon exchange processes.

8.3. *Beyond two sources*

A number of natural and agricultural environments have significant understory vegetation, such as in savannas containing tree-grass ecosystems (Andreu et al., 2018b) or, in the case with agriculture, cover crops deployed for nutrient management and improving soil carbon uptake and soil health (Villat and Nicholas 2024). One of the first attempts to adapt TSEB to account for understory was by Burchard-Levine et al. (2020), who added seasonal phenological dynamics shifting dominant ET coming from actively transpiring grassland to tree cover in an oak-grass savanna (Dehesa) region in Spain (TSEB-2S). A further modification resulted in a three-source approach (3SEB) accounting for soil, grass (understory) and trees (overstory) (Burchard-Levine et al., 2022b). They found 3SEB outperformed both TSEB and TSEB-2S in tree-grass ecosystems in Europe, Australia and Africa (Burchard-Levine et al., 2022b), and provided T estimates that correlated well with T derived from a machine learning ET partitioning method.

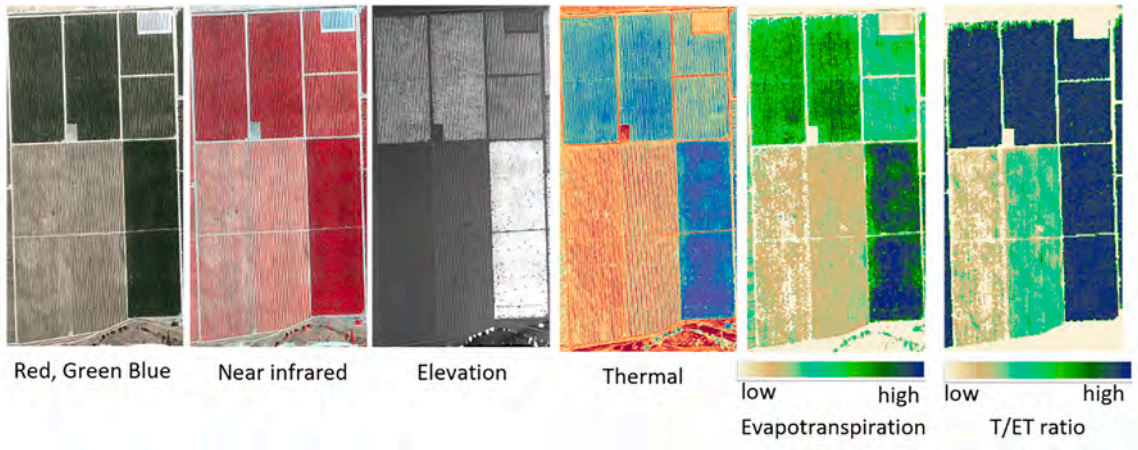

Fig. 15. Example of UAV spectral (red, green, blue), thermal, elevation, daily ET and T/ET ratio data for 0.6 sq miles (422 acres –171 ha) over almond orchards of different age around the OLA T-REX site in Madera Co., CA, using AggieAir UAV drones and TSEB.

Burchard-Levine et al. (2022a) demonstrated 3SEB capacity to partition soil E and T from cover crop and vines, applied over a vineyard with rows managed with and without cover crops.

Future work may need to consider other sources, such as pavement or roof-tops in urban environments.

9. . Conclusions

The Two-Source Energy Balance (TSEB) model was developed in 1995 in response to a set of challenges identified in using remotely sensed LST data for robustly estimating surface fluxes, articulated during the 1993 Workshop in La Londe, France. The primary aim of the original TSEB developers was to create a model that was simple enough to parameterize for large area application, but not too simple such that it ignored fundamental drivers of the relationship between directional surface radiometric temperature and energy partitioning. These drivers include sensor view angle, vegetation cover fraction, differential coupling of the soil and canopy to the atmosphere, and radiation and wind transfer through the canopy.

Through the years, the core TSEB land-surface representation has been integrated into multi-scale ET modeling systems and linked operationally to thermal data collected by GOES, MODIS/VIIRS, Landsat, and the European Sentinel constellation. TSEB-generated ET information is being used to estimate consumptive use, manage irrigation, predict yields, and monitor agricultural drought and ecosystem health within the U.S. and internationally. New sources of thermal imaging and surface reflectance data are continuously integrated into these systems to augment spatial and temporal sampling.

The demonstrated utility of TSEB and other TIR-based SEB modeling systems has transformed community perception of the value of thermal remote sensing as a powerful tool for diagnosing surface water and energy balance over a wide range of spatial scales. Future developments and applications rely on the continued availability of routine global TIR imaging, particularly at Landsat or finer resolution. As more field-scale ET models are implemented in a cloud-based geospatial analysis platform such as GEE, the potential for using an ensemble output may yield generally the most reliable results for regional and global applications (Melton et al., 2022; Jaafar et al., 2022).

CRediT authorship contribution statement

Martha C. Anderson: Writing – original draft, Writing – review & editing, Conceptualization, Methodology, Software, Investigation, Validation. **William P. Kustas:** Writing – original draft, Writing – review & editing, Conceptualization, Methodology, Software, Investigation, Validation. **John M. Norman:** Writing – original draft, Writing – review & editing, Conceptualization, Methodology, Software, Investigation, Validation. **George T. Diak:** Writing – original draft, Writing – review & editing, Conceptualization, Methodology, Software, Investigation, Validation. **Christopher R. Hain:** Writing – review & editing, Methodology, Conceptualization, Software, Investigation, Validation. **Feng Gao:** Writing – review & editing, Methodology, Conceptualization, Software, Investigation, Validation. **Yun Yang:** Writing – review & editing, Methodology, Conceptualization, Software, Investigation, Validation. **Kyle R. Knipper:** Writing – review & editing, Methodology, Conceptualization, Software, Investigation, Validation. **Jie Xue:** Writing – review & editing, Methodology, Conceptualization, Software, Investigation, Validation. **Yang Yang:** Writing – review & editing, Methodology, Conceptualization, Software, Investigation, Validation. **Wade T. Crow:** Writing – review & editing, Methodology, Conceptualization, Software, Investigation, Validation. **Thomas R.H. Holmes:** Writing – review & editing, Methodology, Conceptualization, Software, Investigation, Validation. **Hector Nieto:** Writing – review & editing, Methodology, Conceptualization, Software, Investigation, Validation. **Radoslaw Guzinski:** Writing – review & editing, Methodology, Conceptualization, Software, Investigation, Validation. **Jason A. Otkin:** Writing – review & editing, Methodology, Conceptualization, Software, Investigation, Validation. **John R. Mecikalski:** Writing – review & editing, Methodology, Conceptualization, Software, Investigation, Validation. **Carmelo Cammalleri:** Writing – review & editing, Methodology, Conceptualization, Software, Investigation, Validation. **Alfonso T. Torres-Rua:** Writing – review & editing, Methodology, Conceptualization, Software, Investigation, Validation. **Xiwu Zhan:** Writing – review & editing, Methodology, Conceptualization, Software, Investigation, Validation. **Li Fang:** Writing – review & editing, Methodology, Conceptualization, Software, Investigation, Validation. **Paul D. Colaizzi:** Writing – review & editing, Methodology, Conceptualization, Software, Investigation, Validation. **Nurit Agam:** Writing – review & editing, Methodology, Conceptualization, Software, Investigation, Validation.

Declaration of competing interest

The authors declare the following financial interests/personal relationships which may be considered as potential competing interests:

Martha Anderson reports financial support was provided by NASA. If there are other authors, they declare that they have no known competing financial interests or personal relationships that could have appeared to influence the work reported in this paper.

Data availability

Data will be made available on request.

Acknowledgements

The authors would like to acknowledge the contributions of many others who have contributed to the development of the TSEB modeling systems through the years, including Mahyar Aboutalebi, John Albertson, Ana Andreu, Nico Bambach, Giacomo Bertoldi, Nishan Bhattarai, Claire Brenner, Vicente Burchard-Levine, Elisabet Carpintero, Minha Choi, Jordi Cristobal, Milan Fischer, Andrew French, Rui Gao, María Pat González-Dugo, Rasmus Houborg, Karen Humes, Hadi Jafaar, Yanghui Kang, Arnon Karnieli, Dilia Kool, Fuqin Li, Yan Li, Karem Meza, Christopher Neale, Juan Manuel Sánchez, Kate Semmens, Liesheng Song, Liang Sun, Wim Timmermans, and Mirek Trnka. We would also like to thank the two anonymous reviewers whose thoughtful comments helped to greatly improve the manuscript. USDA is an equal opportunity provider and employer.

References

Aboutalebi, M., Torres-Rua, A.F., Kustas, W.P., Nieto, H., Coopmans, C., McKee, M., 2019. Assessment of different methods for shadow detection in high-resolution optical imagery and evaluation of shadow impact on calculation of NDVI, and evapotranspiration. Irrig. Sci. 37, 407–429.

Aboutalebi, M., Torres-Rua, A.F., McKee, M., Kustas, W.P., Nieto, H., Alsina, M.M., White, A., Prueger, J.H., McKee, L., Alfieri, J., Hipps, L., Coopmans, C., Sanchez, L., Dokoozlian, N., 2022. Downscaling UAV land surface temperature using a coupled wavelet-machine learning-optimization algorithm and its impact on evapotranspiration. Irrig. Sci. 40, 553–574.

Agam, N., Evett, S.R., Tolk, J.A., Kustas, W.P., Colaizzi, P.D., Alfieri, J.G., McKee, L.G., Copeland, K.S., Howell, T.A., Chávez, J.L., 2012. Evaporative loss from irrigated interrows in a highly advective semi-arid agricultural area. Adv. Water Resour. 50, 20–30.

Agam, N., Kustas, W.P., Anderson, M.C., Li, F., Neale, C.M.U., 2007. A vegetation index based technique for spatial sharpening of thermal imagery. Remote Sens. Environ. 107, 545–558.

Agam, N., Kustas, W.P., Anderson, M.C., Norman, J.M., Colaizzi, P.D., Prueger, J.H., 2010. Application of the Priestley-Taylor approach in a two-source surface energy balance model. J. Hydrometeorol. 11, 185–198.

Aguirre-García, S.D., Aranda-Barranco, S., Nieto, H., Serrano-Ortiz, P., Sánchez-Cañete, E.P., Guerrero-Rascado, J.L., 2021. Modelling actual evapotranspiration using a two source energy balance model with Sentinel imagery in herbaceous-free and herbaceous-cover Mediterranean olive orchards. Agric. For. Meteorol. 311. https://doi.org/10.1016/j.agrformet.2021.108692.

Allen, R.G., Tasumi, M., Trezza, R., 2007. Satellite-based energy balance for mapping evapotranspiration with internalized calibration (METRIC) - Model. J. Irrig. Drainage Eng. https://doi.org/10.1061/(ASCE)0733-9437(2007)133:4(380.

Anderson, M.C., Allen, R.G., Morse, A., Kustas, W.P., 2012. Use of Landsat thermal imagery in monitoring evapotranspiration and managing water resources. Remote Sens. Environ. 122, 50–65.

Anderson, M.C., Diak, G.R., Gao, F., Knipper, K., Hain, C.R., Eichelmann, E., Hemes, K.S., Baldocchi, D.D., Kustas, W.P., Yang, Y., 2019. Impact of insolation data source on remote sensing retrievals of evapotranspiration over the California Delta. Remote. Sens. 11, 216.

Anderson, M.C., Gao, F., Knipper, K., Hain, C., Dulaney, W., Baldocchi, D.D., Eichelmann, E., Hemes, K.S., Yang, Y., Medellín-Azuara, J., Kustas, W.P., 2018. Field-scale assessment of land and water use change over the California Delta using remote sensing. Remote. Sens. 10, 889.

Anderson, M.C., Hain, C.R., Jurecka, F., Trnka, M., Hlavinka, P., Dulaney, W., Otkin, J. A., Johnson, D., Gao, F., 2016a. Relationships between the Evaporative Stress Index and winter wheat and spring barley yield anomalies in the Czech Republic. Clim. Res. 70, 215–230.

Anderson, M.C., Hain, C.R., Otkin, J.A., Zhan, X., Mo, K.C., Svoboda, M., Wardlow, B., Pimstein, A., 2013. An intercomparison of drought indicators based on thermal remote sensing and NLDAS-2 simulations with U.S. Drought Monitor classifications. J. Hydrometeorol. 14, 1035–1056.

Anderson, M.C., Hain, C.R., Wardlow, B., Mecikalski, J.R., Kustas, W.P., 2011. Evaluation of drought indices based on thermal remote sensing of evapotranspiration over the continental U.S. J. Clim. 24, 2025–2044.

Anderson, M.C., Norman, J.M., Diak, G.R., Kustas, W.P., Mecikalski, J.R., 1997. A two-source time-integrated model for estimating surface fluxes using thermal infrared remote sensing. Remote Sens. Environ. 60, 195–216.

Anderson, M.C., Norman, J.M., Kustas, W.P., Houborg, R., Starks, P.J., Agam, N., 2008. A thermal-based remote sensing technique for routine mapping of land-surface carbon, water and energy fluxes from field to regional scales. Remote Sens. Environ. 112, 4227–4241.

Anderson, M.C., Norman, J.M., Kustas, W.P., Li, F., Prueger, J.H., Mecikalski, J.M., 2005. Effects of vegetation clumping on two-source model estimates of surface energy fluxes from an agricultural landscape during SMACEX. J. Hydrometeorol. 6, 892–909.

Anderson, M.C., Norman, J.M., Mecikalski, J.R., Otkin, J.A., Kustas, W.P., 2007a. A climatological study of evapotranspiration and moisture stress across the continental U.S. based on thermal remote sensing: II. Surface moisture climatology. J. Geophys. Res. 112, D11112. https://doi.org/10.11029/12006JD007507.

Anderson, M.C., Norman, J.M., Mecikalski, J.R., Otkin, J.A., Kustas, W.P., 2007b. A climatological study of evapotranspiration and moisture stress across the continental U.S. based on thermal remote sensing: I. Model formulation. J. Geophys. Res. 112, D10117. https://doi.org/10.1029/2006JD007506.

Anderson, M.C., Norman, J.M., Mecikalski, J.R., Torn, R.D., Kustas, W.P., Basara, J.B., 2004. A multi-scale remote sensing model for disaggregating regional fluxes to micrometeorological scales. J. Hydrometeor. 5, 343–363.

Anderson, M.C., Yang, Y., Xue, J., Knipper, K.R., Yang, Y., Gao, F., Hain, C.R., Kustas, W. P., Cawse-Nicholson, K., Hulley, G., Fisher, J.B., Alfieri, J.G., Meyers, T.P., Prueger, J., Baldocchi, D.D., Rey-Sanchez, C., 2021. Interoperability of ECOSTRESS and Landsat for mapping evapotranspiration time series at sub-field scales. Remote Sens. Environ. 252.

Anderson, M.C., Zolin, C., Hain, C.R., Semmens, K.A., Yilmaz, M.T., Gao, F., 2015. Comparison of satellite-derived LAI and precipitation anomalies over Brazil with a thermal infrared-based Evaporative Stress Index for 2003-2013. J. Hydrol. https://doi.org/10.1016/j.jhydrol.2015.1001.1005.

Anderson, M.C., Zolin, C., Sentelhas, P.C., Hain, C.R., Semmens, K.A., Yilmaz, M.T., Gao, F., Otkin, J.A., Tetrault, R., 2016b. The Evaporative Stress Index as an indicator of agricultural drought in Brazil: an assessment based on crop yield impacts. Remote Sens. Environ. 174, 82–99.

Andreu, A., Kustas, W.P., Polo, M.J., Carrara, A., González-Dugo, M.P., 2018a. Modeling surface energy fluxes over a dehesa (oak savanna) ecosystem using a thermal based two source energy balance model (TSEB) II-Integration of remote sensing medium and low spatial resolution satellite images. Remote Sens. 10. https://doi.org/10.3390/rs10040558.

Andreu, A., Kustas, W.P., Polo, M.J., Carrara, A., González-Dugo, M.P., 2018b. Modeling surface energy fluxes over a dehesa (oak savanna) ecosystem using a thermal based two-source energy balance model (TSEB) I. Remote Sens. 10. https://doi.org/10.3390/rs10040567.

Andreu, A., Timmermans, W.J., Skokovic, D., Gonzalez-Dugo, M.P., 2015. Influence of component temperature derivation from dual angle thermal infrared observations on TSEB flux estimates over an irrigated vineyard. Acta Geophys. 63, 1540–1570.

Bambach, N., Knipper, K., McElrone, A., Nocco, M., Torres-Rua, A., Kustas, W., Anderson, M.C., Castro, S., Edwards, E., Duran-Gomez, M., Gal, A., Tolentino, P., Wright, I., Roby, M., Gao, F., Alfieri, J., Prueger, J., Hipps, L., Saa, S., 2024. A Tree-crop Remote sensing of Evapotranspiration eXperiment (T-REX): a science-based path for sustainable water management and climate mitigation. Bull. Amer. Meteorol. Soc. in press.

Bartholic, J.T., Namkin, L.N., Wiegand, C.L., 1972. Aerial thermal scanner to determine temperatures of soils and of crop canopies differing in water stress. Agron. J. 64, 603–608.

Bastiaanssen, W.G.M., Menenti, M., Feddes, R.A., Holtslag, A.A.M., 1998. A remote sensing surface energy balance algorithm for land (SEBAL); 1. Formulation. J. Hydrol. 212-213, 198–212.

Blyth, E.M., Dolman, A.J., 1995. The roughness length for heat of sparse vegetation. J. Appl. Meteorol. 34, 583–585.

Brown, K.W., 1974. Calculations of evapotranspiration from crop surface temperature. Agric. Meteorol. 14, 199–209.

Brutsaert, W. (1982). Evaporation Into the atmosphere: theory, History and Applications. Dordrecht, Holland: D. Reidel.

Brutsaert, W., Sugita, M., 1996. Sensible heat transfer parameterization for surfaces with anisothermal dense vegetation. J. Atmos. Sci. 53, 209–216.

Burchard-Levine, V., Nieto, H., Kustas, W.P., Gao, F., Alfieri, J.G., Prueger, J.H., Hipps, L. E., Bambach-Ortiz, N., McElrone, A.J., Castro, S.J., Alsina, M.M., McKee, L.G., Zahn, E., Bou-Zeid, E., Dokoozlian, N., 2022a. Application of a remote-sensing three-source energy balance model to improve evapotranspiration partitioning in vineyards. Irrig. Sci. 40, 593–608.

Burchard-Levine, V., Nieto, H., Riaño, D., Kustas, W.P., Migliavacca, M., El-Madany, T.S., Nelson, J.A., Andreu, A., Carrara, A., Beringer, J., Baldocchi, D., Martín, M.P., 2022b. A remote sensing-based three-source energy balance model to improve global estimations of evapotranspiration in semi-arid tree-grass ecosystems. Glob. Chang. Biol. 28, 1493–1515.

Burchard-Levine, V., Nieto, H., Riaño, D., Migliavacca, M., El-Madany, T.S., Guzinski, R., Carrara, A., Martín, M.P., 2021. The effect of pixel heterogeneity for remote sensing based retrievals of evapotranspiration in a semi-arid tree-grass ecosystem. Remote Sens. Environ. 260. https://doi.org/10.1016/j.rse.2021.112440.

Burchard-Levine, V., Nieto, H., Riaño, D., Migliavacca, M., El-Madany, T.S., Perez-Priego, O., Carrara, A., Martín, M.P., 2020. Seasonal adaptation of the thermal-based two-source energy balance model for estimating evapotranspiration in a semiarid tree-grass ecosystem. Remote Sens. 12. https://doi.org/10.3390/rs12060904.

Cammalleri, C., Anderson, M.C., Ciraolo, G., D'Urso, G., Kustas, W.P., La Loggia, G., Minacapilli, M., 2010. The impact of in-canopy wind profile formulations on heat flux estimation in an open orchard canopy using the remote sensing-based two-source model. Hydrol. Earth Syst. Sci. 14, 2643–2659.

Cammalleri, C., Anderson, M.C., Gao, F., Hain, C.R., Kustas, W.P., 2013. A data fusion approach for mapping daily evapotranspiration at field scale. Water Resour. Res. 49, 1–15. https://doi.org/10.1002/wrcr.20349.

Cammalleri, C., Anderson, M.C., Gao, F.H., R, C., Kustas, W.P, 2014a. Mapping daily evapotranspiration at field scales over rainfed and irrigated agricultural areas using remote sensing data fusion. Agric. For. Meteorol. 186, 1–11.

Cammalleri, C., Anderson, M.C., Kustas, W.P., 2014b. Upscaling of evapotranspiration fluxes from instantaneous to daytime scales for thermal remote sensing applications. Hydrol. Earth Syst. Sci. 18, 1885–1894.

Cammalleri, C., Ciraolo, G., 2012. State and parameter update in a coupled energy/hydrologic balance model using ensemble Kalman filtering. J. Hydrol. 416-417, 171–181.

Carlson, T.N., Dodd, J.K., Benjamin, S.G., Cooper, J.N., 1981. Satellite estimation of the surface energy balance, moisture availability and thermal inertia. J. Appl. Meteorol. 20, 67–87.

Carlson, T.N., Perry, E.M., Schmugge, T.J., 1990. Remote estimation of soil moisture availability and fractional vegetation cover for agricultural fields. Agric. For. Meteorol. 52, 45–69.

Carlson, T.N., Taconet, O., Vidal, A., Gillies, R.R., Olioso, A., Humes, K., 1995. An overview of the workshop on thermal remote sensing held at La Londe les Maures, France, September 20-24, 1993. Agric. For. Meteorol. 77, 141–151.

Castellvi, F., Stockle, C.O., Perez, P.J., Ibanez, M., 2001. Comparison of methods for applying the Priestley-Taylor equation at a regional scale. Hydrol. Process 15, 1609–1620.

Chehbouni, A., Lo Seen, D., Njoku, E.G., Monteny, B., 1996. Examination of the difference between radiometric and aerodynamic surface temperatures over sparsely vegetated surfaces. Remote Sens. Environ. 58, 177–186.

Chen, F., Lei, F., Knipper, K., Gao, F., McKee, L., del Mar Alsina, M., Alfieri, J., Anderson, M., Bambach, N., Castro, S.J., McElrone, A.J., Alstad, K., Dokoozlian, N., Greifender, F., Kustas, W., Notarnicola, C., Agam, N., Prueger, J.H., Hipps, L.E., Crow, W.T., 2022. Application of the Vineyard Data Assimilation (VIDA) system to vineyard root-zone soil moisture monitoring in the California Central Valley. Irrig. Sci. 40, 779–799.

Chintala, S., Harmya, T.S., Kambhammettu, B.V.N.P., Moharana, S., Duvvuri, S., 2022. Modelling high-resolution evapotranspiration in fragmented croplands from the constellation of sentinels. Remote Sens. Appl. 26 https://doi.org/10.1016/j.rsase.2022.100704.

Colaizzi, P.D., Agam, N., Tolk, J.A., Evett, S.R., Howell, T.A., Gowda, P.H., O'Shaughnessy, S.A., Kustas, W.P., Anderson, M.C., 2014. Two-source energy balance model to calculate E, T, and ET: comparison of priestley-taylor and penman-monteith formulations and two time scaling methods. Trans. ASABE 57, 479–498.

Colaizzi, P.D., Agam, N., Tolk, J.A., Evett, S.R., Howell, T.A., O'Shaughnessy, S.A., Gowda, P.H., Kustas, W.P., Anderson, M.C., 2016a. Advances in a two-source energy balance model: partitioning of evaporation and transpiration for cotton. Trans. ASABE 59, 181–197.

Colaizzi, P.D., Evett, S.R., Agam, N., Schwartz, R.C., Kustas, W.P., 2016b. Soil heat flux calculation for sunlit and shaded surfaces under row crops: 1. Model development and sensitivity analysis. Agric. For. Meteorol. 216, 115–128.

Colaizzi, P.D., Evett, S.R., Agam, N., Schwartz, R.C., Kustas, W.P., Cosh, M.H., McKee, L., 2016c. Soil heat flux calculation for sunlit and shaded surfaces under row crops: 2. Model test. Agric. For. Meteorol. 216, 129–140.

Colaizzi, P.D., Evett, S.R., Howell, T.A., Li, F., Kustas, W.P., Anderson, M.C., 2012a. Radiation model for row crops: I. Geometric view factors and parameter optimization. Agron. J. 104, 225–240.

Colaizzi, P.D., Kustas, W.P., Anderson, M.C., Agam, N., Tolk, J.A., Evett, S.R., Howell, T. A., Gowda, P.H., O'Shaughnessy, S.A, 2012b. Two-source energy balance model estimates of evapotranspiration using component and composite surface temperatures. Adv. Water Resour. 50, 134–151.

Corbari, C., Timmermans, W., Andreu, A., 2015. Intercomparison of surface energy fluxes estimates from the FEST-EWB and TSEB models over the heterogeneous REFLEX 2012 site (Barrax, Spain). Acta Geophys. 63, 1609–1638.
Cristóbal, J., Prakash, A., Anderson, M.C., Kustas, W.P., Alfieri, J.G., Gens, R., 2020. Surface energy flux estimation in two boreal settings in Alaska using a thermal-based remote sensing model. Remote Sens. 12, 1–24.
Cristóbal, J., Prakash, A., Anderson, M.C., Kustas, W.P., Euskirchen, E.S., Kane, D.L., 2017. Estimation of surface energy fluxes in the Arctic tundra using the remote sensing thermal-based Two-Source Energy Balance model. Hydrol. Earth Syst. Sci. 21, 1339–1358.
Crow, W.T., Gomez, C.A., Sabater, J.M., Holmes, T., Hain, C.R., Lei, F., Dong, J., Alfieri, J.G., Anderson, M.C., 2020. Soil moisture–evapotranspiration overcoupling and L-band brightness temperature assimilation: sources and forecast implications. J. Hydrometeorol. 21, 2359–2374.
Crow, W.T., Li, F., Kustas, W.P., 2005. Intercomparison of spatially distributed models for predicting surface energy flux patterns during SMACEX. J. Hydrometeorol. 941–953.
De Santis, D., D'Amato, C., Bartkowiak, P., Azimi, S., Castelli, M., Rigon, R., Massari, C., 2022. Evaluation of remotely-sensed evapotranspiration datasets at different spatial and temporal scales at forest and grassland sites in Italy. In: Proceedings of the 2022 IEEE Workshop on Metrology for Agriculture and Forestry, MetroAgriFor 2022 - Proceedings, pp. 356–361.
Diak, G.R., 1990. Evaluation of heat flux, moisture flux and aerodynamic roughness at the land surface from knowledge of the PBL height and satellite-derived skin temperatures. Agric. For. Meteorol. 52, 181–198.
Diak, G.R., Stewart, T.R., 1989. Assessment of surface turbulent fluxes using geostationary satellite surface skin temperatures and a mixed layer planetary boundary layer scheme. J. Geophys. Res. 94, 6357–6373.
Diak, G.R., Whipple, M.S., 1993. Improvements to models and methods for evaluating the land-surface energy balance and 'effective' roughness using radiosonde reports and satellite-measured skin temperature data. Agric. For. Meteor. 63, 189–218.
Diak, G.R., Whipple, M.S., 1994. A note on the use of radiosonde data to estimate the daytime fluxes of sensible and latent heat: a comparison with surface flux measurements from the FIFE. Agric. For. Meteorol. 68, 63–75.
Dong, J., Dirmeyer, P.A., Lei, F., Anderson, M.C., Holmes, T.R.H., Hain, C., Crow, W.T., 2020. Soil evaporation stress determines soil moisture-evapotranspiration coupling strength in land surface modeling. Geophys. Res. Lett. 47. https://doi.org/10.1029/2020GL090391.
Dong, J., Lei, F., Crow, W.T., 2022. Land transpiration-evaporation partitioning errors responsible for modeled summertime warm bias in the central United States. Nat. Commun. 13 https://doi.org/10.1038/s41467-021-27938-6.
Donlon, C., Berruti, B., Buongiorno, A., Ferreira, M.H., Féménias, P., Frerick, J., Goryl, P., Klein, U., Laur, H., Mavrocordatos, C., Nieke, J., Rebhan, H., Seitz, B., Stroede, J., Sciarra, R., 2012. The Global Monitoring for Environment and Security (GMES) Sentinel-3 mission. Remote Sens. Environ. 120, 37–57.
Drusch, M., Del Bello, U., Carlier, S., Colin, O., Fernandez, V., Gascon, F., Hoersch, B., Isola, C., Laberinti, P., Martimort, P., Meygret, A., Spoto, F., Sy, O., Marchese, F., Bargellini, P, 2012. Sentinel-2: eSA's optical high-resolution mission for GMES operational services. Remote Sens. Environ. 120, 25–36.
Evett, S.R., Kustas, W.P., Gowda, P.H., Anderson, M.C., Prueger, J.H., Howell, T.A., 2012. Overview of the Bushland Evapotranspiration and Agricultural Remote sensing EXperiment 2008 (BEAREX08): a field experiment evaluating methods quantifying ET at multiple scales. Adv. Water Resour. 50, 4–19.
Fang, L., Zhan, X., Kalluri, S., Yu, P., Hain, C., Anderson, M., Laszlo, I., 2022. Application of a machine learning algorithm in generating an evapotranspiration data product from coupled thermal infrared and microwave satellite observations. Front. Big Data 5. https://doi.org/10.3389/fdata.2022.768676.
Fang, L., Zhan, X., Schull, M., Kalluri, S., Laszlo, I., Yu, P., Carter, C., Hain, C., Anderson, M., 2019. Evapotranspiration data product from NESDIS GET-D system upgraded for GOES-16 ABI observations. Remote Sens. 11. https://doi.org/10.3390/rs11222639.
Fisher, J.B., Melton, F.S., Middleton, E.M., Hain, C.R., Anderson, M.C., Allen, R.G., McCabe, M.F., Hook, S., Baldocchi, D.D., Townsend, P.A., Kilic, A., Tu, K., Miralles, D.D., Perret, J., Lagouarde, J.P., Waliser, D., Purdy, A.J., French, A.N., Schimel, D., Famiglietti, J.S., Stephens, G., Wood, E.F., 2017. The future of evapotranspiration: global requirements for ecosystem functioning, carbon and climate feedbacks, agricultural management, and water resources. Water Resour. Res. 53, 2618–2626.
Gao, F., Kustas, W.P., Anderson, M.C., 2012. A data mining approach for sharpening thermal satellite imagery over land. Remote Sens. 4, 3287–3319.
Gao, F., Masek, J., Schwaller, M., Hall, F.G., 2006. On the blending of the Landsat and MODIS surface reflectance: predicting daily Landsat surface reflectance. IEE Trans. Geosci. Remote. Sens. 44, 2207–2218.
Gao, R., Torres-Rua, A.F., Aboutalebi, M., White, W.A., Anderson, M., Kustas, W.P., Agam, N., Alsina, M.M., Alfieri, J., Hipps, L., Dokoozlian, N., Nieto, H., Gao, F., McKee, L.G., Prueger, J.H., Sanchez, L., McElrone, A.J., Bambach-Ortiz, N., Coopmans, C., Gowing, I., 2022. LAI estimation across California vineyards using sUAS multi-seasonal multi-spectral, thermal, and elevation information and machine learning. Irrig. Sci. https://doi.org/10.1007/s00271-022-00776-0.
Gao, R., Torres-Rua, A.F., Nieto, H., Zahn, E., Hipps, L., Kustas, W.P., Alsina, M.M., Bambach, N., Castro, S.J., Prueger, J.H., Alfieri, J., McKee, L.G., White, W.A., Gao, F., McElrone, A.J., Anderson, M., Knipper, K., Coopmans, C., Gowing, I., Agam, N., Sanchez, L., Dokoozlian, N., 2023. ET partitioning assessment using the TSEB model and sUAS information across California Central Valley Vineyards. Remote Sens. 15 https://doi.org/10.3390/rs15030756.
García-Santos, V., Sánchez, J.M., Cuxart, J., 2022. Evapotranspiration acquired with remote sensing thermal-based algorithms: a state-of-the-art review. Remote Sens. 14. https://doi.org/10.3390/rs14143440.
Garrat, J.G., Hicks, B.B., 1973. Momentum, heat and water vapor transfer to and from natural and artificial surfaces. Quart. J. Roy. Meteorolog. Soc. 99, 680–687.
Gillies, R.R., Carlson, T.N., Cui, J., Kustas, W.P., Humes, K.S., 1997. A verification of the "triangle" method for obtaining surface soil water content and energy fluxes from remote measurements of the Normalized Difference Vegetation Index (NDVI) and surface radiant temperature. Int. J. Remote Sens. 18, 3145–3166.
Guzinski, R., Anderson, M.C., Kustas, W.P., Nieto, H., Sandholt, I., 2013. Using a thermal-based two source energy balance model with time-differencing to estimate surface energy fluxes with day-night MODIS observations. Hydrol. Earth Syst. Sci. 17, 2809–2825.
Guzinski, R., Nieto, H., 2019. Evaluating the feasibility of using Sentinel-2 and Sentinel-3 satellites for high-resolution evapotranspiration estimations. Remote Sens. Environ. 221, 157–172.
Guzinski, R., Nieto, H., Ramo Sánchez, R., Sánchez, J.M., Jomaa, I., Zitouna-Chebbi, R., Roupsard, O., López-Urrea, R., 2023. Improving field-scale crop actual evapotranspiration monitoring with Sentinel-3, Sentinel-2, and Landsat data fusion. Int. J. Appl. Earth Obs. Geoinf. 125. https://doi.org/10.1016/j.jag.2023.103587.
Guzinski, R., Nieto, H., Sanchez, J.M., Lopez-Urrea, R., Boujnah, D.M., Boulet, G., 2021. Utility of copernicus-based inputs for actual evapotranspiration modeling in support of sustainable water use in agriculture. IEEE J. Selected Topics Appl. Earth Observ. Remote Sens. 14, 11466–11484.
Guzinski, R., Nieto, H., Sandholt, I., Karamitilios, G., 2020. Modelling high-resolution actual evapotranspiration through Sentinel-2 and Sentinel-3 data fusion. Remote Sens. 12. https://doi.org/10.3390/RS12091433.
Haigh, T.R., Otkin, J.A., Mucia, A., Hayes, M., Burbach, M.E., 2019. Drought early sarning and the timing of range managers' drought response. Adv. Meteorol. https://doi.org/10.1155/2019/9461513, 2019.
Hain, C.R., Anderson, M.C., 2017. Estimating morning changes in land surface temperature from MODIS day/night observations: applications for surface energy balance modeling. Geophys. Res. Lett. 44, 9723–9733.
Hain, C.R., Crow, W.T., Anderson, M.C., Mecikalski, J.R., 2012. Developing a dual assimilation approach for thermal infrared and passive microwave soil moisture retrievals. Water Resour. Res. 48, W11517. https://doi.org/10.1029/2011WR011268.
Hain, C.R., Crow, W.T., Anderson, M.C., Yilmaz, M.T., 2015. Diagnosing neglected soil moisture source/sink processes via a thermal infrared-based Two-Source Energy Balance model. J. Hydrometeorol. 16, 1070–1086.
Hain, C.R., Crow, W.T., Mecikalski, J.R., Anderson, M.C., Holmes, T., 2011. An intercomparison of available soil moisture estimates from thermal-infrared and passive microwave remote sensing and land-surface modeling. J Geophys. Res. 116, D15107. https://doi.org/10.1029/2011JD015633.
Hain, C.R., Mecikalski, J.R., Anderson, M.C., 2009. Retrieval of an available water-based soil moisture proxy from thermal infrared remote sensing. Part I: methodology and validation. J. Hydrometeorol. 10, 665–683.
Hall, F.G., Huemmrich, K.F., Goetz, S.J., Sellers, P.J., Nickerson, J.E., 1992. Satellite remote sensing of surface energy balance: success, failures and unresolved issues in FIFE. J. Geophys. Res. 97, 19, 061-019,089.
Hobbins, M.T., Wood, A., McEvoy, D.J., Huntington, J.L., Morton, C., Anderson, M., Hain, C., 2016. The evaporative demand drought index. Part I: linking drought evolution to variations in evaporative demand. J. Hydrometeorol. 17, 1745–1761.
Holmes, T., Crow, W.T., Hain, C.R., Anderson, M.C., Kustas, W.P., 2015. Diurnal temperature cycle as observed by thermal infrared and microwave radiometers. Remote Sens. Environ. 158, 110–125.
Holmes, T., Hain, C., Crow, W., Anderson, M.C., Kustas, W.P., 2018. Microwave implementation of two-source energy balance approach for estimating evapotranspiration. Hydrol. Earth Syst. Sci. 22, 1351–1369.
Holmes, T.R.H., De Jeu, R.A.M., Owe, M., Dolman, A.J., 2009. Land surface temperature from Ka band (37GHz) passive microwave observations. J. Geophys. Res. Atmos. 114 https://doi.org/10.1029/2008JD010257.
Holmes, T.R.H., Hain, C.R., Anderson, M.C., Crow, W.T., 2016. Cloud tolerance of remote-sensing technologies to measure land surface temperature. Hydrol. Earth Syst. Sci. 20, 3263–3275.
Houborg, R., Anderson, M.C., Daughtry, C.S.T., Kustas, W.P., Rodell, M., 2011. Using leaf chlorophyll to parameterize light-use-efficiency within a thermal-based carbon, water and energy exchange model. Remote Sens. Environ. 115, 1694–1705.
Houborg, R., Soegaard, H., Boegh, E., 2007. Combining vegetation index and model inversion methods for the extraction of key vegetation biophysical parameters using Terra and Aqua MODIS reflectance data. Remote Sens. Environ. 106, 39–58.
Idso, S.B., Jackson, R.D., Pinter Jr, P.J., Reginato, R.J., Hatfield, J.L, 1981. Normalizing the stress-degree-day parameter for environmental variability. Agric. Meteorol. 24, 45–55.
Idso, S.B., Jackson, R.D., Reginato, R.J., 1977. Remote-sensing of crop yields. Science 196, 19–25.
Irons, J.R., Dwyer, J.L., Barsi, J.A., 2012. The next landsat satellite; the landsat data continuity mission. Remote Sens. Environ. 122, 11–21.
Isaacson, B.N., Yang, Y., Anderson, M.C., Clark, K.L., Grabosky, J.C., 2023. The effects of forest composition and management on evapotranspiration in the New Jersey Pinelands. Agric. For. Meteorol. 339. https://doi.org/10.1016/j.agrformet.2023.109588.
Jaafar, H.H., Mourad, R.M., Kustas, W.P., Anderson, M.C., 2022. A global implementation of single- and dual-source surface energy balance models for estimating actual evapotranspiration at 30-m resolution using Google Earth Engine. Water Resour. Res. 58 https://doi.org/10.1029/2022WR032800.

Jackson, R.D., Idso, S.B., Reginato, R.J., Pinter, P.J., 1981. Canopy temperature as a crop water stress indicator. Water Resour. Res. 4, 1133–1138.
Jackson, R.D., Kustas, W.P., Choudhury, B.J., 1988. A reexamination of the crop water stress index. Irrig. Sci. 9, 309–317.
Jackson, R.D., Reginato, R.J., Idso, S.B., 1977. Wheat canopy temperature: a practical tool for evaluating water requirements. Water Resour. Res. 13, 651–656.
Jurečka, F., Fischer, M., Hlavinka, P., Balek, J., Semerádová, D., Bláhová, M., Anderson, M.C., Hain, C., Žalud, Z., Trnka, M., 2021. Potential of water balance and remote sensing-based evapotranspiration models to predict yields of spring barley and winter wheat in the Czech Republic. Agric. Water Manage. 256. https://doi.org/10.1016/j.agwat.2021.107064.
Kang, Y., Gao, F., Anderson, M., Kustas, W., Nieto, H., Knipper, K., Yang, Y., White, W., Alfieri, J., Torres-Rua, A., Alsina, M.M., Karnieli, A., 2022. Evaluation of satellite Leaf Area Index in California vineyards for improving water use estimation. Irrig. Sci. 40, 531–551.
Khan, A.M., Stoy, P.C., Douglas, J.T., Anderson, M., Diak, G., Otkin, J.A., Hain, C., Rehbein, E.M., McCorkel, J., 2021. Reviews and syntheses: ongoing and emerging opportunities to improve environmental science using observations from the advanced baseline imager on the geostationary operational environmental satellites. Biogeosciences 18, 4117–4141.
Knipper, K., Anderson, M., Bambach, N., Kustas, W., Gao, F., Zahn, E., Hain, C., McElrone, A., Belfiore, O.R., Castro, S., Alsina, M.M., Saa, S., 2023. Evaluation of partitioned evaporation and transpiration estimates within the DisALEXI modeling framework over irrigated crops in California. Remote Sens. 15. https://doi.org/10.3390/rs15010068.
Knipper, K., Kustas, W.P., Anderson, M.C., Alsina, M., Hain, C., Alfieri, J.G., Prueger, J., Gao, F., McKee, L., Sanchez, L.A., 2019. Using high-spatiotemporal thermal satellite ET retrievals for operational water use and stress monitoring in a California vineyard. Remote. Sens. 11, 2124.
Knipper, K.R., Kustas, W.P., Anderson, M.C., Nieto, H., Alfieri, J.G., Prueger, J.H., Hain, C.R., Gao, F., McKee, L.G., Alsina, M., Sanchez, L., 2020. Using high-spatiotemporal thermal satellite ET retrievals to monitor water use over California vineyards of different climate, vine variety and trellis design. Water Resour. Res. 241, 106361.
Kool, D., Agam, N., Lazarovitch, N., Heitman, J.L., Sauer, T.J., Ben-Gal, A., 2014. A review of approaches for evapotranspiration partitioning. Agric. For. Meteorol. 184, 56–70.
Kool, D., Kustas, W.P., Ben-Gal, A., Agam, N., 2021. Energy partitioning between plant canopy and soil, performance of the two-source energy balance model in a vineyard. Agric. For. Meteorol. 300. https://doi.org/10.1016/j.agrformet.2021.108328.
Koster, R.D., Feldman, A.F., Holmes, T.R.H., Anderson, M.C., Crow, W.T., Hain, C., 2024. Estimating hydrological regimes from observational soil moisture, evapotranspiration, and air temperature data. J. Hydrometeorol. in press.
Kustas, W.P., 1990. Estimates of evapotranspiration with a one- and two-layer model of heat transfer over partial canopy cover. J. Appl. Meteorol. 29, 704–715.
Kustas, W.P., Alfieri, J.G., Anderson, M.C., Colaizzi, P.D., Prueger, J.H., Neale, C.M.U., French, A.N., Hipps, L.E., Chavez, J.L., Copeland, K.S., Howell, T.A., 2012. Evaluating the two-source energy balance model using local thermal and surface flux observations in a strongly advective irrigated agricultural area. Adv. Water Resour. 50, 120–133.
Kustas, W.P., Alfieri, J.G., Nieto, H., Wilson, T.G., Gao, F., Anderson, M.C., 2019. Utility of the two-source energy balance (TSEB) model in vine and interrow flux partitioning over the growing season. Irrig. Sci. 37, 375–388.
Kustas, W.P., Anderson, M.C., 2009. Advances in thermal infrared remote sensing for land surface modeling. Agric. For. Meteorol. 149, 2071–2081.
Kustas, W.P., Anderson, M.C., Alfieri, J.G., Knipper, K., Torres-Rua, A., Parry, C.K., Nieto, H., Agam, N., White, A., Gao, F., McKee, L., Prueger, J.H., Hipps, L.E., Los, S. O., Alsina, M., Sanchez, L., Sams, B., Dokoozlian, N., McKee, M., Jones, S., McElrone, A., Heitman, J.L., Howard, A.M., Post, K., Melton, F.S., Hain, C., 2018. The Grape Remote sensing Atmospheric Profile and Evapotranspiration eXperiment (GRAPEX). Bull. Amer. Meteorol. Soc. 99, 1791–1812.
Kustas, W.P., Choudhury, B.J., Moran, M.S., Reginato, R.D., Jackson, R.D., Gay, L.W., Weaver, H.L., 1989. Determination of sensible heat flux over sparse canopy using thermal infrared data. Agric. For. Meteorol. 44, 197–216.
Kustas, W.P., Daughtry, C.S.T., 1990. Estimation of the soil heat flux/net radiation ratio from spectral data. Agric. For. Meteorol. 49, 205–223.
Kustas, W.P., Diak, G.R., Norman, J.M., 2001. Time difference methods for monitoring regional scale heat fluxes with remote sensing. Land Surf. Hydrol. Meteorol. Climate 3, 15–29.
Kustas, W.P., Humes, K.S., Norman, J.M., Moran, M.S., 1996. Single- and dual-source modeling of surface energy fluxes with radiometric surface temperature. J. Appl. Meteorol. 35, 110–121.
Kustas, W.P., Nieto, H., Garcia-Tejera, O., Bambach, N., McElrone, A.J., Gao, F., Alfieri, J.G., Hipps, L.E., Prueger, J.H., Torres-Rua, A., Anderson, M.C., Knipper, K., Alsina, M.M., McKee, L.G., Zahn, E., Bou-Zeid, E., Dokoozlian, N., 2022. Impact of advection on two-source energy balance (TSEB) canopy transpiration parameterization for vineyards in the California Central Valley. Irrig. Sci. https://doi.org/10.1007/s00271-022-00778-y.
Kustas, W.P., Nieto, H., Morillas, L., Anderson, M.C., Alfieri, J.G., Hipps, L.E., Villagarcía, L., Domingo, F., Garcia, M., 2016. Revisiting the paper "Using radiometric surface temperature for surface energy flux estimation in Mediterranean drylands from a two-source perspective. Remote Sens. Environ. 184, 645–653.
Kustas, W.P., Norman, J.M., 1996. Use of remote sensing for evapotranspiration monitoring over land surfaces. Hydrol. Sci. J. 41, 495–516.
Kustas, W.P., Norman, J.M., 1999a. Reply to comments about the basic equations of dual-source vegetation-atmosphere transfer models. Agric. For. Meteorol. 94, 275–278.
Kustas, W.P., Norman, J.M., 1999b. Evaluation of soil and vegetation heat flux predictions using a simple two-source model with radiometric temperatures for partial canopy cover. Agric. For. Meteorol. 94, 13–29.
Kustas, W.P., Norman, J.M., 2000. A two-source energy balance approach using directional radiometric temperature observations for sparse canopy covered surfaces. Agronomy J. 92, 847–854.
Kustas, W.P., Norman, J.M., Anderson, M.C., French, A.N., 2003. Estimating subpixel surface temperatures and energy fluxes from the vegetation index-radiometric temperature relationship. Remote Sens. Environ. 85, 429–440.
Lei, F., Crow, W.T., Holmes, T.R.H., Hain, C., Anderson, M.C., 2018. Global investigation of soil moisture and latent heat flux coupling strength. Water Resour. Res. 54, 8196–8215.
Lei, F., Crow, W.T., Kustas, W.P., Dong, J., Yang, Y., Knipper, K.R., Anderson, M.C., Gao, F., Notarnicola, C., Greifeneder, F., McKee, L.M., Alfieri, J.G., Hain, C., Dokoozlian, N., 2020. Data assimilation of high-resolution thermal and radar remote sensing retrievals for soil moisture monitoring in a drip-irrigated vineyard. Remote Sens. Environ. 239. https://doi.org/10.1016/j.rse.2019.111622.
Leuning, R., 1995. A critical appraisal of a combined stomatal-photosynthesis model for C_3 plants. Plant Cell Environ. 18, 339–355.
Lhomme, J.P., Monteny, B., Amadou, M., 1994. Estimating sensible heat flux from radiometric temperature over sparse millet. Agric. For. Meteorol. 68, 77–91.
Lhomme, J.P., Troufleau, D., Monteny, B., Chehbouni, A., Baudin, S., 1997. Sensible heat flux and radiometric surface temperature over sparse Sahelian vegetation II: a model for the kB-1 parameter. J. Hydrol. 188-189, 839–854.
Li, Y., Kustas, W.P., Huang, C., Kool, D., Haghighi, E., 2018. Evaluation of soil resistance formulations for estimates of sensible heat flux in a desert vineyard. Agric. For. Meteorol. 255–261, 260-261.
Li, Y., Kustas, W.P., Huang, C., Nieto, H., Haghighi, E., Anderson, M.C., Domingo, F., Garcia, M., Scott, R.L., 2019. Evaluating soil resistance formulations in thermal-based Two-Source Energy Balance (TSEB) model: implications for heterogeneous semiarid and arid regions. Water Resour. Res. https://doi.org/10.1029/2018WR022981.
Mahrt, L., Sun, J., Pederson, J.R., Desjardin, R.L., 1997. Formulation of the surface temperature for prediction of heat flux: application to BOREAS. J. Geophys. Res. 102, 641–649.
Matsushima, D., Kondo, J., 1997. A proper method for estimating sensible heat flux above a horizontal-homogeneous vegetation canopy using radiometric surface observations. J. Appl. Meteorol. 36, 1696–1711.
McNaughton, K.G., Spriggs, T.W., 1986. A mixed-layer model for regional evaporation. Boundary-Layer Meteorol. 74, 262–288.
Mecikalski, J.M., Diak, G.R., Anderson, M.C., Norman, J.M., 1999. Estimating fluxes on continental scales using remotely-sensed data in an atmosphere-land exchange model. J. Applied Meteorol. 38, 1352–1369.
Melton, F.S., Huntington, J., Grimm, R., Herring, J., Hall, M., Rollison, D., Erickson, T., Allen, R., Anderson, M., Fisher, J.B., Kilic, A., Senay, G.B., Volk, J., Hain, C., Johnson, L., Ruhoff, A., Blankenau, P., Bromley, M., Carrara, W., Daudert, B., Doherty, C., Dunkerly, C., Friedrichs, M., Guzman, A., Halverson, G., Hansen, J., Harding, J., Kang, Y., Ketchum, D., Minor, B., Morton, C., Ortega-Salazar, S., Ott, T., Ozdogan, M., ReVelle, P.M., Schull, M., Wang, C., Yang, Y., Anderson, R.G., 2022. OpenET: filling a critical data gap in water management for the Western United States. J. Am. Water Resour. Assoc. 58, 971–994.
Menzel, W.P., Schmit, T.J., Zhang, P., Li, J., 2018. Satellite-based atmospheric infrared sounder development and applications. Bull. Am. Meteorol. Soc. 99, 583–603.
Merlin, O., Chehbouni, A., 2004. Different approaches in estimating heat flux using dual angle observations of radiative surface temperature. Int. J. Remote Sens. 25, 275–289.
Minacapilli, M., Agnese, C., Blanda, F., Cammalleri, C., Ciraolo, G., D'Urso, G., Iovino, M., Pumo, D., Provenzano, G., Rallo, G., 2009. Estimation of actual evapotranspiration of Mediterranean perennial crops by means of remote-sensing based surface energy balance models. Hydrol. Earth Syst. Sci. 13, 1061–1074.
Mishra, V., Cruise, J.F., Mecikalski, J.R., 2021. Assimilation of coupled microwave/thermal infrared soil moisture profiles into a crop model for robust maize yield estimates over Southeast United States. Eur. J. Agron. 123. https://doi.org/10.1016/j.eja.2020.126208.
Mladenova, I.E., Bolten, J.D., Crow, W.T., Anderson, M.C., Hain, C.R., Johnson, D.M., Mueller, R., 2017. Intercomparison of soil moisture, evaporative stress and vegetation indices for estimating corn and soybean yields over the U.S. J. Selected Topics Appl. Earth Obs. Remote Sens. 10, 1328–1343.
Monteith, J.L., 1995. A reinterpretation of stomatal responses to humidity. Plant Cell Environ. 18, 357–364.
Monteith, J.L., Szeicz, G., 1962. Radiative temperature in the heat balance of natural surfaces. Q. J. R. Meteorolog. Soc. 88, 496–507.
Moran, M.S., 2003. Thermal infrared measurement as an indicator of plant ecosystem health. In: Quattrochi, D.A., Luvall, J. (Eds.), Thermal Remote Sensing in Land Surface Processes. Taylor and Francis, pp. 257–282.
Nieto, H., Alsina, M.M., Kustas, W.P., García-Tejera, O., Chen, F., Bambach, N., Gao, F., Alfieri, J.G., Hipps, L.E., Prueger, J.H., McKee, L.G., Zahn, E., Bou-Zeid, E., McElrone, A.J., Castro, S.J., Dokoozlian, N., 2022. Evaluating different metrics from the thermal-based two-source energy balance model for monitoring grapevine water stress. Irrig. Sci. 40, 697–713.
Nieto, H., Kustas, W.P., Torres-Rúa, A., Alfieri, J.G., Gao, F., Anderson, M.C., White, W. A., Song, L., Alsina, M.M., Prueger, J.H., McKee, M., Elarab, M., McKee, L.G., 2019. Evaluation of TSEB turbulent fluxes using different methods for the retrieval of soil

and canopy component temperatures from UAV thermal and multispectral imagery. Irrig. Sci. 37, 389–406.
Norman, J.M., 1979. Modeling the complete crop canopy. In: Barfield, B.J., Gerber, J.F. (Eds.), Modification of the Aerial Environment of Plants. Amer. Soc. Agric. Eng, MI, pp. 249–277. St. Joseph.
Norman, J.M., Anderson, M.C., Kustas, W.P., French, A.N., Mecikalski, J.R., Torn, R.D., Diak, G.R., Schmugge, T.J., Tanner, B.C.W., 2003. Remote sensing of surface energy fluxes at 10^1-m pixel resolutions. Water Resour. Res. 39, 1221.
Norman, J.M., Becker, F., 1995. Terminology in thermal infrared remote sensing of natural surfaces. Remote Sens. Rev. 12, 159–173.
Norman, J.M., Campbell, G., 1983. Application of a plant-environment model to problems in irrigation. In: Hillel, D. (Ed.), Advances in Irrigation. Academic Press, New York, pp. 156–188.
Norman, J.M., Divakarla, M., Goel, N.S., 1995a. Algorithms for extracting information from remote thermal-IR observations of the earth's surface. Remote Sens. Environ. 51, 157–168.
Norman, J.M., Kustas, W.P., Humes, K.S., 1995b. A two-source approach for estimating soil and vegetation energy fluxes from observations of directional radiometric surface temperature. Agric. For. Meteorol. 77, 263–293.
Norman, J.M., Kustas, W.P., Prueger, J.H., Diak, G.R., 2000. Surface flux estimation using radiometric temperature: a dual temperature difference method to minimize measurement error. Water Resour. Res. 36, 2263–2274.
Norman, J.M., Russell, G., Marshall, B., Jarvis, P., 1988. Synthesis of canopy processes. In: Plant Canopies: Their Growth, Form and Function, Soc. Exp. Biol., Seminar Series, 31. Cambridge University Press, New York, pp. 161–175.
Otkin, J.A., Anderson, M.C., Hain, C., Svoboda, M., Johnson, D., Mueller, R., Tadesse, T., Wardlow, B., Brown, J., 2016. Assessing the evolution of soil moisture and vegetation conditions during the 2012 United States flash drought. Agric. For. Meteorol. 218-219, 230–242.
Otkin, J.A., Anderson, M.C., Hain, C.R., Mladenova, I.E., Basara, J.B., Svoboda, M., 2013. Examining rapid onset drought development using the thermal infrared based Evaporative Stress Index. J. Hydrometeorol. 14, 1057–1074.
Otkin, J.A., Anderson, M.C., Hain, C.R., Svoboda, M., 2014. Examining the relationship between drought development and rapid changes in the Evaporative Stress Index. J. Hydrometeorol. https://doi.org/10.1175/JHM-D-13-0110.1.
Otkin, J.A., Anderson, M.C., Hain, C.R., Svoboda, M., 2015a. Using temporal changes in drought indices to generate probabilistic drought intensification forecasts. J. Hydrometeorol. 16, 88–105.
Otkin, J.A., Haigh, T., Mucia, A., Anderson, M.C., Hain, C., 2018a. Comparison of agricultural stakeholder survey results and drought monitoring datasets during the 2016U.S. Northern Plains flash drought. Weather Climate Soc. 10, 867–883.
Otkin, J.A., Shafer, M., Svoboda, M., Wardlow, B., Anderson, M.C., Hain, C.R., Basara, J. B., 2015b. Facilitating the use of drought warning information through interactions with agricultural stakeholders. Bull. Amer. Meteorol. Soc. 96, 1073–1078.
Otkin, J.A., Svoboda, M., Hunt, E.D., Ford, T.W., Anderson, M.C., Hain, C., Basara, J.B., 2018b. Flash droughts: a review and assessment of the challenges imposed by rapid-onset droughts in the United States. Bull. Am. Meteorol. Soc. 99, 911–919.
Otkin, J.A., Woloszyn, M., Wang, H., Svoboda, M., Skumanich, M., Pulwarty, R., Lisonbee, J., Hoell, A., Hobbins, M., Haigh, T., Cravens, A.E., 2022. Getting ahead of flash drought: from early warning to early action. Bull. Am. Meteorol. Soc. 103, E2188–E2202.
Otkin, J.A., Zhong, Y., Hunt, E.D., Basara, J.B., Svoboda, M., Anderson, M.C., Hain, C., 2019. Assessing the evolution of soil moisture and vegetation conditions during a flash drought - flash recovery sequence over the South-Central United States. J. Hydrometeorol. 20, 549–562.
Otkin, J.A., Zhong, Y., Lorenz, D., Anderson, M.C., Hain, C., 2018c. Exploring seasonal and regional relationships between the Evaporative Stress Index and surface weather and soil moisture anomalies across the United States. Hydrol. Earth Syst. Sci. 22, 5373–5386.
Owen, P.R., Thomson, W.R., 1963. Heat transfer across rough surfaces. J. Fluid Mech. 15, 321–334.
Peng, J., Nieto, H., Neumann Andersen, M., Kørup, K., Larsen, R., Morel, J., Parsons, D., Zhou, Z., Manevski, K., 2023. Accurate estimates of land surface energy fluxes and irrigation requirements from UAV-based thermal and multispectral sensors. ISPRS J. Photogramm. Remote Sens. 198, 238–254.
Perico, R., Brunner, P., Frattini, P., Crosta, G.B., 2022. Water balance in Alpine catchments by Sentinel data. Water Resour. Res. 58 https://doi.org/10.1029/2021WR031355.
Price, J.C., 1980. The potential of remotely sensed thermal infrared data to infer surface soil moisture and evaporation. Water Resourc. Res. 16, 787–795.
Priestley, C.H.B., Taylor, R.J., 1972. On the assessment of surface heat flux and evaporation using large-scale parameters. Mon. Weather Rev. 100, 81–92.
Sanchez, J.M., Galve, J.M., Nieto, H., Guzinski, R., 2024. Assessment of high-resolution LST derived from the synergy of sentinel-2 and sentinel-3 in agricultural areas. IEEE J. Selected Topics Appl. Earth Observ. Remote Sens. 17, 916–928.
Santanello, J.A., Friedl, M.A., 2003. Diurnal variation in soil heat flux and net radiation. J. Appl. Meteorol. 42, 851–862.
Scanlon, T.M., Kustas, W.P., 2010. Partitioning carbon dioxide and water vapor fluxes using correlation analysis. Agric. For. Meteorol. 150, 89–99.
Scanlon, T.M., Kustas, W.P., 2012. Partitioning evapotranspiration using an eddy covariance-based technique: improved assessment of soil moisture and land-atmosphere exchange dynamics. Vadose Zone J. 11. https://doi.org/10.2136/vzj2012.0025.
Scanlon, T.M., Sahu, P., 2008. On the correlation structure of water vapor and carbon dioxide in the atmospheric surface layer: a basis for flux partitioning. Water Resour. Res. 44. https://doi.org/10.1029/2008WR006932.
Schull, M.A., Anderson, M.C., Houborg, R., Gitelson, A., Kustas, W.P., 2015. Thermal-based modeling of coupled carbon, water and energy fluxes using nominal light use efficiencies constrained by leaf chlorophyll observations. Biogeosciences 12, 1151–1523.
Sellers, P.J., Hall, F.G., Asrar, G., Strebel, D.E., Murphy, R.E., 1988. The First ISLSCP Field Experiment (FIFE). Bull. Amer. Meteorol. Soc. 69, 22–27.
Semmens, K.A., Anderson, M.C., Kustas, W.P., Gao, F., Alfieri, J.G., McKee, L., Prueger, J. H., Hain, C.R., Cammalleri, C., Yang, Y., Xia, T., Vélez, M., Sanchez, L., Alsina, M., 2016. Monitoring daily evapotranspiration over two California vineyards using Landsat 8 in a multi-sensor data fusion approach. Remote Sens. Environ. https://doi.org/10.1016/j.rse.2015.1010.1025.
Shuttleworth, W.J., Gurney, R.J., 1990. The theoretical relationship between foliage temperature and canopy resistance in sparse crop. Quart. J. Roy. Meteorolog. Soc. 116, 497–519.
Shuttleworth, W.J., Wallace, J.S., 1985. Evaporation from sparse crops - an energy combination theory. Q. J. Royal Meteorol. Soc. 111, 839–855.
Stewart, J.B., Kustas, W.P., Humes, K.S., Nichols, W.D., Moran, M.S., DeBruin, A.A.R., 1994. Sensible heat flux-radiometric surface temperature relationship for eight semiarid areas. J. Appl. Meteorol. 33, 1110–1117.
Stocker, B.D., Tumber-Dávila, S.J., Konings, A.G., Anderson, M.C., Hain, C., Jackson, R. B., 2023. Global patterns of water storage in the rooting zones of vegetation. Nat. Geosci. 16, 250–256.
Sun, J., Mahrt, L., 1995. Determination of surface fluxes from the surface radiative temperature. J. Atmospheric Sci. 52, 1096–1106.
Sun, J., Massman, W., Grantz, D.A., 1999. Aerodynamic variables in the bulk formulation of turbulent fluxes. Boundary Layer Meteorol. 91, 109–125.
Sun, L., Anderson, M.C., Gao, F., Hain, C.R., Alfieri, J.G., Sharifi, A., McCarty, G., Yang, Y., Yang, Y., 2017. Investigating water use over the Choptank River Watershed using a multi-satellite data fusion approach. Water Resources Res 53, 5298–5319.
Taconet, O., Carlson, T., Bernard, R., Vidal-Madjar, D., 1986. Evaluation of a surface/vegetation parameterization using satellite measurements of surface temperature. J. Clim. Appl. Meteorol. 25, 1752–1767.
Tanner, C.B., 1963. Plant temperatures. Agron. J. 55, 201–211.
Tanner, C.B., Jury, W.A., 1976. Estimating evaporation and transpiration from a row crop during incomplete cover. Agron. J. 68, 239–242.
Trnka, M., Hlavinka, P., Možný, M., Semerádová, D., Štěpánek, P., Balek, J., Bartošová, L., Zahradníček, P., Bláhová, M., Skalák, P., Farda, A., Hayes, M., Svoboda, M., Wagner, W., Eitzinger, J., Fischer, M., Žalud, Z., 2020. Czech Drought Monitor System for monitoring and forecasting agricultural drought and drought impacts. Int. J. Climatol. 40, 5941–5958.
Troufleau, D., Lhomme, J.P., Monteny, B., Vidal, A., 1997. Sensible heat flux and radiometric surface temperature over sparse Sahelian vegetation. I. An experimental analysis of the kB-1 parameter. J. Hydrol. 815–838, 188-189.
Vanderleest, C.P.L., Bland, W.L., 2016. Evapotranspiration from cranberry compared with the equilibrium rate. Can. J. Soil Sci. 97, 5–10.
Verhoef, A., De Bruin, H.A.R., van den Hurk, B.J.J.M, 1997. Some practical notes on the parameter kB^{-1} for sparse vegetation. J. Appl. Meteorol. 36, 560–572.
Villat, J., Nicholas, K.A., 2024. Quantifying soil carbon sequestration from regenerative agricultural practices in crops. Front. Sustainable Food Syst. 7, 1234108.
Vining, R.C., Blad, B.L., 1992. Estimation of sensible heat flux from remotely sensed canopy temperatures. J. Geophys. Res. 97 (D17), 954, 18,951-918.
Volk, J.M., Huntington, J., Melton, F.S., Allen, R., Anderson, M.C., Fisher, J.B., Kilic, A., Ruhoff, A., Senay, G., Minor, B., Morton, C., Ott, T., Johnson, L., Andrade, B., Carrara, W., Doherty, C., Dunkerly, C., Friedrichs, M., Guzman, A., Hain, C., Halverson, G., Kang, Y., Knipper, K., Laipelt, L., Ortega-Salazar, S., Pearson, C., Parrish, G., Purdy, A.J., Revelle, P., Wang, T., Yang, Y., 2024. Assessing the accuracy of OpenET satellite-baswed data to support water resource and land management applications. Nature Water in press.
Walker, C., 2023. Evaluation of Atmospheric Land Exchange Inverse Model Evaporative Stress Index Utilizing Soil Climate Analysis Network Stations in Alabama. The University of Alabama in Huntsville, p. 136.
Wetzel, P.J., Atlas, D., Woodward, R., 1984. Determining soil moisture from geosynchronous satellite infrared data: a feasibility study. J. Clim. Appl. Meteorol. 23, 375–391.
Xue, J., Anderson, M.C., Gao, F., Hain, C., Knipper, K.R., Yang, Y., Kustas, W.P., Yang, Y., Bambach, N., McElrone, A.J., Castro, S.J., Alfieri, J.G., Prueger, J.H., McKee, L.G., Hipps, L.E., del Mar Alsina, M., 2022. Improving the spatiotemporal resolution of remotely sensed ET information for water management through Landsat, Sentinel-2, ECOSTRESS and VIIRS data fusion. Irrig. Sci. 40, 609–634.
Xue, J., Anderson, M.C., Gao, F., Hain, C., Sun, L., Yang, Y., Knipper, K.R., Kustas, W.P., Torres-Rua, A., Schull, M.A., 2020. Sharpening ECOSTRESS and VIIRS land surface temperature using harmonized Landsat-Sentinel surface reflectance. Remote Sens. Environ. 251, 112055.
Xue, J., Anderson, M.C., Gao, F., Hain, C., Yang, Y., Knipper, K.R., Kustas, W.P., Yang, Y., 2021. Mapping daily evapotranspiration at field scale using the Harmonized Landsat and Sentinel-2 dataset, with sharpened VIIRS as a Sentinel-2 thermal proxy. Remote Sens. 13. https://doi.org/10.3390/rs13173420.
Yang, Y., Anderson, M., Gao, F., Hain, C., Noormets, A., Sun, G., Wynne, R., Thomas, V., Sun, L., 2020. Investigating impacts of drought and disturbance on evapotranspiration over a forested landscape in North Carolina, USA using high spatiotemporal resolution remotely sensed data. Remote Sens. Environ. 238, 111018.
Yang, Y., Anderson, M., Gao, F., Xue, J., Knipper, K., Hain, C., 2022. Improved daily evapotranspiration estimation using remotely sensed data in a data fusion system. Remote Sens. 14. https://doi.org/10.3390/rs14081772.

Yang, Y., Anderson, M.C., Gao, F., Hain, C., Kustas, W.P., Meyers, T., Crow, W., Finocchiaro, R.G., Otkin, J.A., Sun, L., Yang, Y., 2017a. Impact of tile drainage on evapotranspiration (ET) in South Dakota, USA based on high spatiotemporal resolution ET timeseries from a multi-satellite data fusion system. J. Selected Topics Appl. Earth Obs. Remote Sens. 10, 2550–2564.

Yang, Y., Anderson, M.C., Gao, F., Hain, C.R., Semmens, K.A., Kustas, W.P., Normeets, A., Wynne, R.H., Thomas, V.A., Sun, G., 2017b. Daily Landsat-scale evapotranspiration estimation over a managed pine plantation in North Carolina, USA using multi-satellite data fusion. Hydrol. Earth Syst. Sci. 21, 1017–1037.

Yang, Y., Anderson, M.C., Gao, F., Johnson, D.M., Yang, Y., Sun, L., Dulaney, W., Hain, C. R., Otkin, J.A., Prueger, J., Meyers, T.P., Bernacchi, C.J., Moore, C.E., 2021a. Phenological corrections to a field-scale, ET-based crop stress indicator: an application to yield forecasting across the U.S. Corn Belt. Remote Sens. Environ. 257, 112337.

Yang, Y., Anderson, M.C., Gao, F., Wardlow, B., Hain, C.R., Otkin, J.A., Alfieri, J., Yang, Y., Sun, L., Dulaney, W., 2018. Field-scale mapping of evaporative stress indicators of crop yield: an application over Mead, NE, USA. Remote Sens. Environ. 210, 387–402.

Yang, Y., Anderson, M.C., Gao, F., Wood, J.D., Gu, L., Hain, C., 2021b. Studying drought-induced forest mortality using high spatiotemporal resolution evapotranspiration data from thermal satellite imaging. Remote Sens. Environ. 265. https://doi.org/10.1016/j.rse.2021.112640.

Yilmaz, M.T., Anderson, M.C., Zaitchik, B.F., Hain, C.R., Crow, W.T., Ozdogan, M., Chung, J.A., 2014. Comparison of prognostic and diagnostic surface flux modeling approaches over the Nile River Basin. Water Resour. Res. 50, 386–408.

Zahn, E., Bou-Zeid, E., Good, S.P., Katul, G.G., Thomas, C.K., Ghannam, K., Smith, J.A., Chamecki, M., Dias, N.L., Fuentes, J.D., Alfieri, J.G., Kwon, H., Caylor, K.K., Gao, Z., Soderberg, K., Bambach, N.E., Hipps, L.E., Prueger, J.H., Kustas, W.P., 2022. Direct partitioning of eddy-covariance water and carbon dioxide fluxes into ground and plant components. Agric. For. Meteorol. 315. https://doi.org/10.1016/j.agrformet.2021.108790.